7.0 An evaluation of the drainage prediction by SWIM

7.1 Introduction

Drainage involves the movement of water from the upper horizons of the soil profile to deeper layers. It is an important process as it controls the quantity of water retained in the plant root zone, the available air-filled porosity for subsequent storage of water and adequate aeration for plant growth, and the recharge of ground water (Ward and Robinson, 1989). The availability of plant nutrients is also influenced by the redistribution of water and some nutrients may be lost by leaching through deep drainage. Therefore a knowledge of profile drainage is an essential component of plant nutrition.

The Soil Water Infiltration and Movement (SWIM) model is a water balance model that can simulate water movement through a given soil and is based on the soil's hydraulic properties (Section 3.3.2). SWIM was developed in Australia and has been successfully used in a number of situations. However, its use in pasture soils has not been evaluated.

Model evaluations are essential to provide confidence in their application. They provide important information as to the validity of the model. That is, how well the model describes certain processes and whether or not model output is realistic. A model evaluation should involve a comparison of simulated output with actual observations and examine the sensitivity of model output to changes in input parameter values (Cresswell *et al.*, 1994).

The aim of this experiment was to evaluate SWIM for its prediction of drainage from a gleyed podzolic soil at Big Ridge 1. The evaluation involved determining the *in situ* hydraulic conductivity function by using a method that involved inverting Richards' equation. Soil hydraulic properties were measured and used as inputs into SWIM which simulated water movement by use of Richards' equation. SWIM's drainage prediction was assessed by comparing simulated and measured profile water contents over time and cumulative drainage. The evaluation also examined the sensitivity of SWIM's drainage prediction to changes in the models inputs.

7.2 Materials and methods

7.2.1 *In situ* measurement of soil hydraulic properties

7.2.1.1 Construction of the drainage plot

A drainage plot was set up outside the boundary of plot 1 on the gleyed podzolic soil (for location, see Figure 4.3). The drainage plot was approximately 6 m from the soil profile pit (Chapter 6). Preparation of the 4 m^2 plot involved excavating a 2 m deep trench around the perimeter in order to lay plastic sheeting down the sides to a depth below the rooting zone (Plate 7.1). The plastic was extended over wooden planks, which were placed around each side of the plot (Plate 7.2). The plastic isolates the plot from any surface and subsurface lateral water flow onto or out of the plots. Once the plastic was laid down on each side of the plot, the trench was backfilled and compacted. The excavated zones were not sufficiently compacted when backfilled, and subsequently did not support the weight of the soil once it was saturated. This resulted in the sides of the excavation partially collapsing and producing some cracking on the plot's surface. However, the cracks were shallow and were not considered to interfere with the workings of any experimental equipment.

Plate 7.1: Plastic was placed around each side of the drainage plot to a depth of 2m

7.2.1.2 Moisture content

An aluminium access tube for a neutron moisture meter (NMM) was installed in the centre of the plot to measure soil water content to a depth of 1.8 m. The installation method was adapted from the 'auguring and reaming an undersized hole' method described by Prebble *et al.* (1981). The hole was excavated by hand using a bucket auger, which fitted inside a soil corer that had an outer diameter just less than the diameter of the NMM access tube. The corer was inserted through a hole in a thick block of timber laid on the surface to keep the hole vertical. The tube was then pushed into the hole by hammering a 'dolly' that was fitted onto the end of the tube to prevent any damage to the tube. At least two NMM counts were taken over 32 seconds at 10 cm intervals to a maximum depth of 1.8 m.

7.2.1.3 Matric potential

Tensiometers were installed in the plot to measure soil matric potential. They were constructed from 20 mm diameter electrical conduit, which was glued to a porous ceramic cup. They were installed at a distance of approximately 0.7 m from the NMM access tube so not to affect water content readings (Plate 7.2). Two sets of tensiometers were placed at depths of 20, 40, 60, 80, 100, 120, 140 and 180 cm.

Plate 7.2: Layout of the drainage plot

Prior to installation the tensiometers were tested to ensure that they had no leaks. This involved soaking the cups in water overnight and then applying a 60-80 kPa positive pressure to the tensiometer with the cup and joints immersed in water.

Installation of the tensiometers involved auguring a hole with a bucket auger that had a diameter slightly larger than that of the tensiometer. A small amount of slurry of fine sand was placed at the bottom of the hole. The tensiometer was placed into the hole and the porous cup embedded in the slurry with a twisting motion. Extra sand was added to the height of the ceramic cup to ensure good hydraulic contact between the cup and the surrounding soil. The hole was backfilled around the tensiometer shaft with a mix of finely ground clay soil and bentonite, which was firmly tamped to prevent water running down the sides of the tensiometer. Each tensiometer was connected to a mercury manometer as shown in Plate 7.3.

Plate 7.3: A mercury manometer

As the tensiometers were in close proximity to each other, they were connected to a manometer system, consisting of a wooden box housing a mercury reservoir. Graph paper was attached to the back of the box to facilitate reading of the height of the mercury column. Fine nylon tubing (internal diameter 1.5 mm) was connected to the tensiometers at one end and extended into the mercury reservoir at the other. Tensiometers were filled with de-aerated water and the tubing connecting the tensiometers to the mercury reservoir was de-aired to obtain a water-tight closed system. The system is illustrated in Plate 7.4. As the tensiometers come into equilibrium with the surrounding soil a suction is created so that mercury is drawn up out of the reservoir. The height of mercury corresponds to a certain matric potential, which is calculated using the following equation:

$$\begin{aligned} \psi m &= (1 - d_{hg} / d_w) Z_{hg} + Z_o \\ &= -12.57 Z_{hg} + Z_o \qquad [7.1] \end{aligned}$$

where: d_{hg} is the density of mercury, d_w is the density of water, Z_{hg} is the height of mercury, Z_o is the height of water. These heights are shown in Figure 7.1.

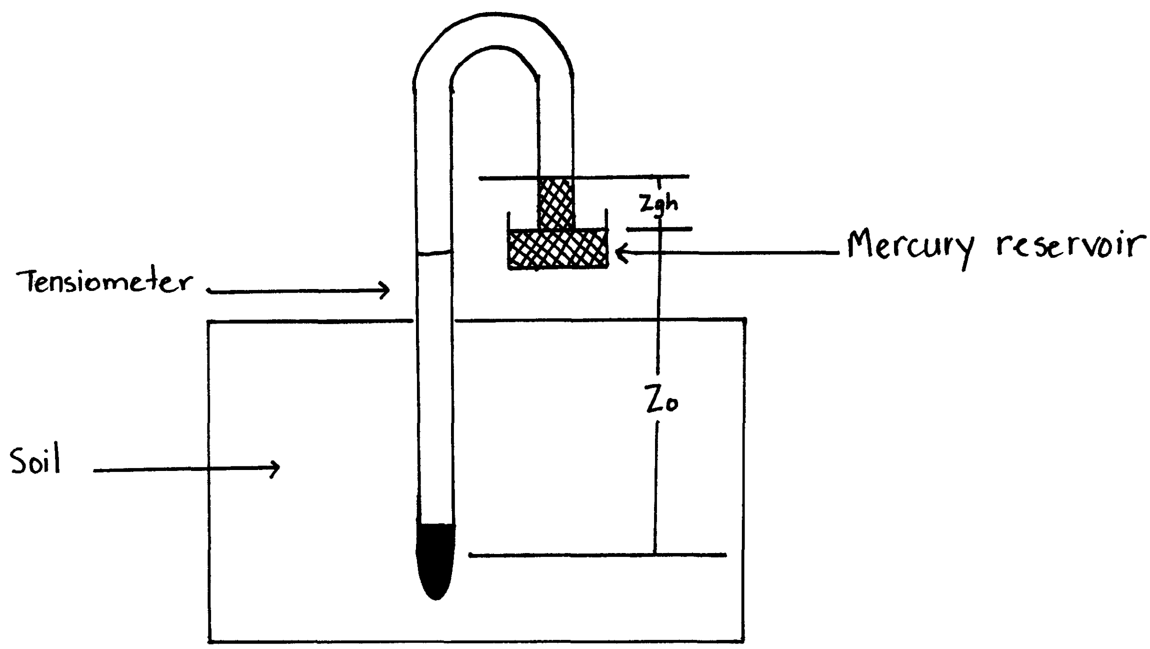

Figure 7.1: Calculation of matric potential using a mercury manometer (Hanks, 1992)

7.2.1.4 Wetting of plots and monitoring change

After installation of the tensiometers and the NMM access tube, the drainage plot was wetted. It was saturated initially by ponding rain water on the soil surface. The rapid wetting resulted in a loss of water down the sides of the plastic sheeting, so that the interior of the plot did not get wetted. This did not affect the useability of this plot. Thereafter a dripper system was used to wet up the soil more slowly. The degree of saturation was monitored by the NMM. At the start of the experiment all tensiometers except those at 160 and 180 cm recorded positive pressures, indicating that the soil was saturated. A sheet of plastic and a layer of mulch were then placed on top of the plot to prevent any evapotranspiration and a tent-like structure was constructed over the plot to prevent wetting by rainfall (Plate 7.4). The plastic sheet was taped securely around each side of the plot as well as around the tensiometers and the NMM access tube to give a complete seal.

As internal drainage proceeded in the soil, the water content and matric potential were measured at various time intervals. Initially measurements were taken at 1, 3, 6, 10, 20 and 28 hours from the starting time when the soil was saturated Thereafter measurements were taken daily for the next week, then once a week for the next month. The time between successive readings was gradually increased over the drainage period with the final measurement taken at about 3000 hours from the starting time.

Plate 7.4: A drainage plot ready for measurements to be taken

7.2.1.5 Moisture characteristic measured ***in situ***

The moisture characteristic was determined from *in situ* matric potential and water content measurements for each depth during drying of the drainage plot.

The change in water content at each depth gradually became smaller over time. This was particularly so at depths greater than 40 cm. Due to the small changes occurring, experimental error sometimes resulted in NMM readings being higher than at the previous time of reading. The size of these errors were very small, at less than a 1 per cent increase in water content. Unfortunately a standard count was not taken immediately before each reading, which should have reduced the error in measurement. Therefore, to reduce noise in NMM readings a regression line was fitted through the water content and time data at the 40 to 120 cm depths. The change in water content was so small at the 130 to 180 cm depths that the regression lines were almost horizontal. Therefore, the average water content over time was calculated for each of these depths and it was assumed that the water content remained constant over the time of the experiment.

7.2.1.6 Hydraulic conductivity function determined ***in situ***

The hydraulic conductivity function, K(θ), was calculated from the continuity equation of water flow. The equation states that the change in water content over time is equal to the change in flux (rate of water flow per unit area) with distance.

$$\frac{\partial \theta}{\partial t} = -\frac{\partial q}{\partial z} \qquad [7.2]$$

where θ = volumetric water content
q = Darcy's soil water flux
t = time
z = depth

Values of soil water flux (q) were calculated from water content data at different depths and different times using the following equation:

$$q(\mathrm{z},\mathrm{t}) = \frac{W(t_1) - W(\mathrm{t}_2)}{(t_1) - (\mathrm{t}_2)} \qquad [7.3]$$

where W(t_1) = total water storage to depth z in the soil profile at time t_1 (time before t_2)
W(t_2) = total water storage to depth z in the soil profile at time t_2.

Matric potential measurements were used to calculate hydraulic gradient (I(z,t)) at depth z and time t from:

$$I(z,t) = (\partial\psi / \partial z) - 1 \qquad [7.4]$$

where ψ = matric potential taken at time t corresponding to depth z.

Given q(z, t) and I(z, t), Darcy's law can be rearranged to calculate unsaturated hydraulic conductivity (K(z,t)) for a given time and depth:

$$K_{(z,t)} = -\frac{q}{\frac{\partial\psi}{\partial z} - 1} \qquad [7.5]$$

For a given soil depth z, water content (θ) and matric potential (ψ) decrease over time during drainage so that K can be expressed either for a range of θ or ψ. This permits the K(θ) and K (ψ) functions to be calculated. These functions were determined for the 40, 60, 80, 100 and 120 cm depths.

There appeared to be some disturbance to drainage after about 286 hours. The data indicated some upward movement of water despite the plot appearing to be well sealed to prevent evaporation and hence upward movement of water. The underside of the plastic cover at the end of the experiment was found to be damp from moisture condensing at the soil surface suggesting that some upward movement had occurred. Therefore, measurements of hydraulic conductivity obtained beyond the 286 hour were discarded.

7.2.1.7 Hydraulic conductivity function predicted from moisture characteristic data

The following model developed by Campbell (1974), described in Section 2.4.2.3, was used to predict unsaturated hydraulic conductivity from the moisture characteristic data:

$$K(\theta) = K_s\left(\frac{\theta}{\theta_s}\right)^m \qquad [7.6]$$

where K(θ) = hydraulic conductivity function

K_S = saturated hydraulic conductivity

θ = soil water content

θs = saturated soil water content

$m = 2b + 3$, b is the best fit line relating θ to ψ on a log-log scale.

The soil parameters required for this model were calculated from the combined laboratory and *in situ* moisture characteristic data (7.2.2.2), except for saturated hydraulic conductivity (K_S), which was measured *in situ* (see Section 7.2.1.6). K_S was assumed to be equal to the conductivity measured at the start of the drainage experiment when the plot was saturated.

Campbell's (1974) hydraulic conductivity function was used to predict $K(\theta)$ for different depths in the soil profile from the moisture characteristic data. The predicted $K(\theta)$ function was compared to the *in situ* $K(\theta)$ function to examine how well it described the K data from the plot in order to parameterise SWIM for the drainage evaluation.

7.2.2 Evaluation of the drainage component of SWIM

7.2.2.1 Model initialisation

The Soil Water Infiltration and Movement (SWIM) model was used to simulate water movement through the gleyed podzolic soil in order to evaluate the model for its prediction of drainage. The inputs used to initialise SWIM are presented in Table 7.1.

The starting time was at 0 hours, the commencement of measurements. At this stage the matric potentials read from the tensiometers at the 40 to 120 cm depths were zero indicating soil saturation. The matric potential at 20 cm depth at time 0 hours was -5.88 cm H_20. The finishing time was at the 286th hour (see section 7.2.1.6) so that the simulation was run over a 286 hour period. During this time it was assumed that there was no transpiration, evaporation or precipitation.

Although the conductance and runoff input parameters have no influence on the draining soil profile, SWIM required some values to enable it to run. Therefore, surface conductance, surface storage and the runoff rate factor and power were set at realistic values for the gleyed podzolic soil type at Big Ridge 1. The precipitation constant and effectiveness parameter under the runoff and conductance menus were set to the model's default values (Ross, 1990a).

The soil profile used in the simulation consisted of six horizontally uniform layers, with hydraulic properties measured at defined intervals to a maximum depth of 120 cm. As outlined in Section 2.3.2, water movement through the soil profile is governed by the soil moisture characteristic and hydraulic conductivity function. SWIM uses the equations of Campbell (1974, 1985) to define these functions and requires the following inputs to parameterise these equations: θs, ψe, b and K_s.

The lower boundary condition assumed drainage out of the 120 cm layer was due to gravity alone. There was a 5 cm space in between layers (node spacing) and SWIM was set to central weighting which meant that the hydraulic properties within the node space were an average of the layer above and below that particular node.
Model predictions of water content at selected times and drainage over time were compared with the values measured in the field in order to evaluate the model for its prediction of drainage.

The simulation described above was also run for 3000 hours to examine the change in water content over an extended time period.

Table 7.1: Inputs used for the SWIM simulation of the drainage plot

(a) Times Data

Parameter	Value
Starting time	0 h
Finishing time	286 h
Print interval	1 h
Water increment	0.01 cm

(b) Surface conductance data

Parameter	Value
Initial soil surface conductance	14 /h
Minimum soil surface conductance	14 /h
Precipitation constant[a]	2.5 cm
Effectiveness parameter[a]	0.184

(c) Runoff data

Parameter	Value
Initial soil surface storage[b]	0.2 cm
Minimum soil surface storage[b]	0.2 cm
Precipitation constant[a]	2.5 cm
Runoff rate factor[c]	2 (cm/h)/cm^p
Runoff rate power[c]	2
Initial surface water depth	0

(d): Soil hydraulic properties

Layer cm	ψ cm H2O	θ_s m/m	ψ_e cm H2O	b	Ks cm/hr	n[d]	Km cm/hr	m[d]
0	-2.88	0.357	-27.04	7.19	8.62	0	0	0
5	-2.88	0.357	-27.04	7.19	8.62	0	0	0
10	-2.88	0.357	-27.04	7.19	8.62	0	0	0
15	-3.96	0.357	-27.04	7.19	8.62	0	0	0
20	-3.96	0.357	-27.04	7.19	8.62	0	0	0
25	-3.96	0.357	-27.04	7.19	8.62	0	0	0
30	-15.07	0.357	-27.04	7.19	8.62	0	0	0
35	-3.43	0.4784	-62.476	13.36	1.891	195	0.173	10
40	-3.43	0.4784	-62.476	13.36	1.891	195	0.173	10
45	-82.32	0.4784	-62.476	13.36	1.891	195	0.173	10
50	-82.32	0.4784	-62.476	13.36	1.891	195	0.173	10
55	-9.67	0.4567	-119.17	11.814	1.523	520	0.13	31
60	-9.67	0.4567	-119.17	11.814	1.523	520	0.13	31
65	-114.33	0.4567	-119.17	11.814	1.523	520	0.13	31
70	-114.33	0.4567	-119.17	11.814	1.523	520	0.13	31
75	-15.88	0.433	-223.59	11.814	0.771	620	0.194	28
80	-15.88	0.433	-223.59	11.814	0.771	620	0.194	28
85	-252.46	0.433	-223.59	11.814	0.771	620	0.194	28
90	-252.46	0.433	-223.59	11.814	0.771	620	0.194	28
95	-14.41	0.4156	-362.64	11.814	1.552	1500	0.104	55
100	-14.41	0.4156	-362.64	11.814	1.552	1500	0.104	55
105	-406.71	0.4156	-362.64	11.814	1.552	1500	0.104	55
110	-406.71	0.4156	-362.64	11.814	1.552	1500	0.104	55
115	-54.78	0.398	-605.56	11.814	0.676	950	0.049	130
120	-54.78	0.398	-605.56	11.814	0.676	950	0.049	130

[a] Ross (1990), [b] Moore and Larson, [c] H. Cresswell *pers. comm.*, [d] Refer equation 7.11

7.2.2.2 Moisture characteristic for SWIM initialisation

As the saturated drainage plot was very slow to drain, the range of *in situ* moisture content and matric potential investigated was narrow, especially in the clay B horizons. All data points at each depth were at the wet end of the curve ($\psi_m > -30$ kPa), and were mostly clustered around the air-entry potential. Consequently it was difficult to fit a line that was representative, particularly at the dry end of the curve. In order to extend the range of the data and thus apply Campbell's function, laboratory data were combined with *in situ* measurements made at the six lowest matric potentials for the 20, 40 and 60 cm depths. Six moisture characteristic points were chosen as this number resulted in the best fit between laboratory and *in situ* moisture characteristic data.

The *in situ* moisture characteristic points at the 20 cm depth did not match the points obtained in the laboratory, for which volumetric moisture content was calculated from soil cores. A better fit was obtained when the laboratory determined gravimetric water content was converted to volumetric using bulk density calculated from saturated water content (θ_S) as measured *in situ*. θ_S was taken as the first reading of water content when matric potential equalled zero. The laboratory determined bulk density at 20 cm depth was 1570 kg m^{-3}, whereas the *in situ* determined bulk density was 1704 kg m^{-3}. This differences could be due to variation in the depth to the B horizon between the drainage plot and the soil profile pit.

Laboratory determined bulk density was used at the 40 and 70 cm depths, as a it resulted in a better relationship between the *in situ* and laboratory determined moisture characteristics. θ_S at the 40 cm and 70 cm depths calculated from the laboratory determined bulk densities was found to differ from the saturated water content measured in the field. By keeping the slopes of the moisture characteristics (b) the same, a new air-entry potential was measured which corresponded to the *in situ* θ_S value (Figure 7.2). This involved calculating a matric potential from its corresponding water content on the moisture characteristic using Campbell's (1974) water retention equation:

$$\psi_m = \psi_e(\theta / \theta_s)^{-b} \qquad [7.7]$$

where ψ_m = matric potential

ψ_e = air entry potential

θ = water content corresponding the matric potential ψ_m

θ_s = saturated water content

b = slope of the best fit line relating θ to ψ on a log-log scale

Campbell's (1974) water retention equation [7.7] was then rearranged to calculate air-entry potential (Equation 7.8). Substituting the moisture characteristic point from equation [7.7] into equation [7.8] with a new θ_S value, its corresponding air-entry potential was determined.

$$\psi_e = \psi_m(\theta / \theta_s)^b \qquad [7.8]$$

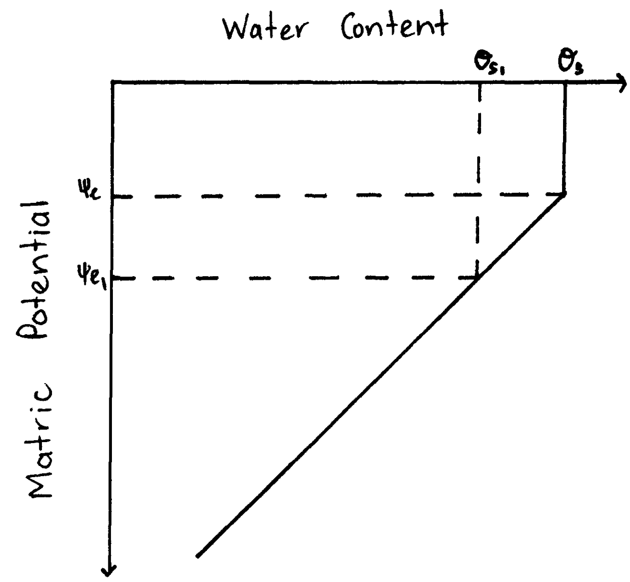

Figure 7.2: Calculation of a new air-entry potential corresponding to a different saturated water content assuming the slope of the moisture characteristic remains the same, where θ_S=laboratory saturated water content and θ_{S1}=*in situ* saturated water content.

SWIM uses the equation of Hutson and Cass (1987) to smooth the wet end of the Campbell's (1974) water retention function. As shown in Figure 7.3, Campbell's (1974) water retention function is exponential having a sharp discontinuity at the air-entry potential ($\psi_e \equiv$ a). The water content equals θ_S over the potential range ψ=0 to ψ_e. In reality soils do not exhibit such abrupt changes in water retention and have sigmoidal retention curves (Hutson and Cass, 1987). Hutson and Cass (1987) suggested that Campbell's (1974) water retention function can be improved by replacing the exponential function with a parabolic function at high water contents.

The equations of Hutson and Cass (1987) describe a two-part water retentivity function (Equations 7.9 and 7.10). SWIM defines initial water potentials based on field values of water content, by using these equations.

At the point of inflection of the parabolic and exponential functions, where $\theta = \theta i$:

$$\theta_i = (2b\theta_s)/(1+2b)$$
$$\psi_i = a((2b)/(1+2b))^{-b} \qquad [7.9]$$

where θi = water content at the point of inflection

b = slope of the best fit line relating θ to ψ on a log-log scale

θ_S = saturated water content

ψ_i = matric potential at the point of inflection

a = air entry potential

At the parabolic portion where $\theta \geq \theta i$ and $\psi \geq \psi i$:

$$\theta = \theta s - \frac{\theta_s \psi^2 (1-\theta_i/\theta_s)}{a^2(\theta_i/\theta_s)^{-2b}}$$
$$\psi = \frac{a(1-\theta/\theta_s)^{1/2}(\theta_i/\theta_s)^{-b}}{(1-\theta_i/\theta_s)^{1/2}} \qquad [7.10]$$

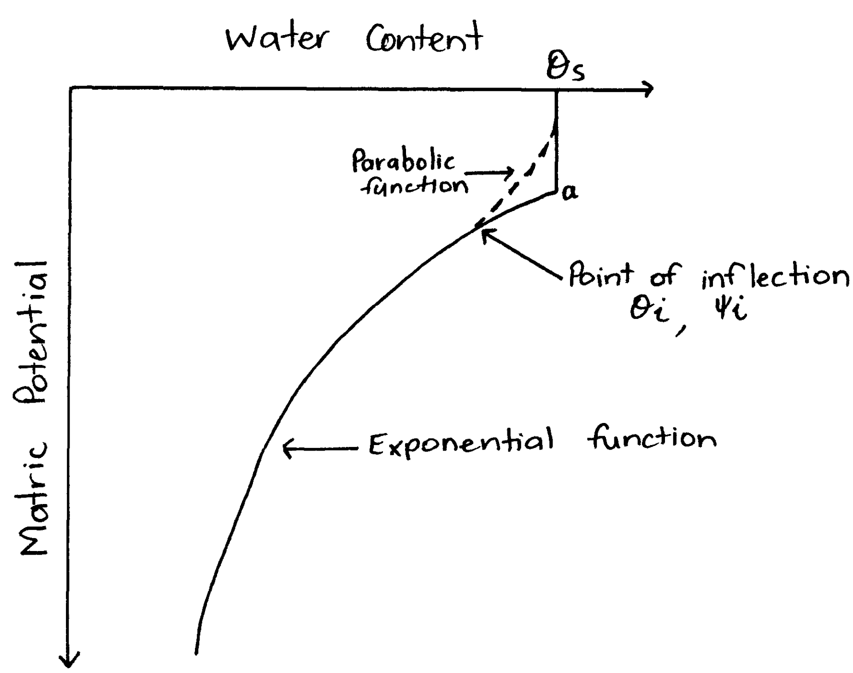

Figure 7.3: Campbell's (1974) water retention function with a parabolic function fitted to the wet end of the curve (Hutson and Cass, 1987)

7.2.2.3 Hydraulic conductivity function for SWIM initialisation

Saturated hydraulic conductivity (K_S) at 20 cm depth was taken to be equal to K at 10 mm tension, measured using a disc permeameter (Section 5.2.3). K_S at the remaining depths was measured *in situ* (Section 7.2.1.6). SWIM uses Campbell's (1974) hydraulic conductivity function to estimate K(θ) from the water retention data. SWIM can also account for initially high flows, usually through macropores, when the soil water content is close to saturation by using a modified Campbell's (1974) equation of the form:

$$K = (K_s(\theta / \theta_s)^{bn}) + (K_m(\theta / \theta_s)^{bm}) \qquad [7.11]$$

where saturated hydraulic conductivity is the sum of K_S and K_m, b is the slope of the moisture characteristic and n and m are constants (Ross 1990). The values of n and m dictate the slope of the K(θ) function. Therefore, SWIM is able to model a function which is initially steep but then flattens out once a certain moisture content has been reached (Figure 7.4). Equation [7.11] described the measured K data better than equation [7.6] and so equation [7.11] was used in the SWIM initialisation (Refer forward to Section 7.3.1.5).

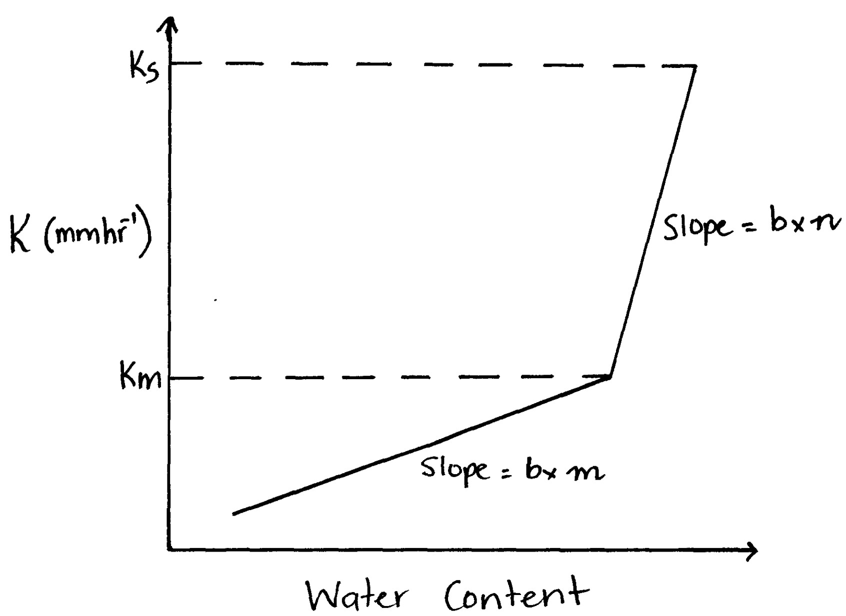

Figure 7.4: A K(θ) function where K is equal to the sum of K_S and K_m.

7.2.2.4 Sensitivity analysis

A linear sensitivity analysis was carried out to determine the sensitivity of SWIM's drainage predictions to changes in the soil input parameters. The sensitivity analysis involved changing each soil parameter $\pm$ 10 % from its base value. The base values are given in Table 7.1. Each soil parameter was changed one at a time, whilst keeping all other inputs at their specified base value. Changes to each soil parameter were made to each layer in the soil profile. The simulations ran for 286 hours. The sensitivity of SWIM output to certain soil inputs was examined by comparing the differences in model output following each simulation.

7.3 Results and discussion

7.3.1 *In situ* measurement of soil hydraulic properties

7.3.1.1 Change in soil water content over time

Figure 7.5 shows the soil profile gradually drying with time. There is very little change in water content over time at depths greater than 30 cm. The sharp increase in water content at 40 cm depth is typical of a duplex soil, indicating the boundary between the sandy clay loam A horizon and the medium to heavy clay textured B horizon.

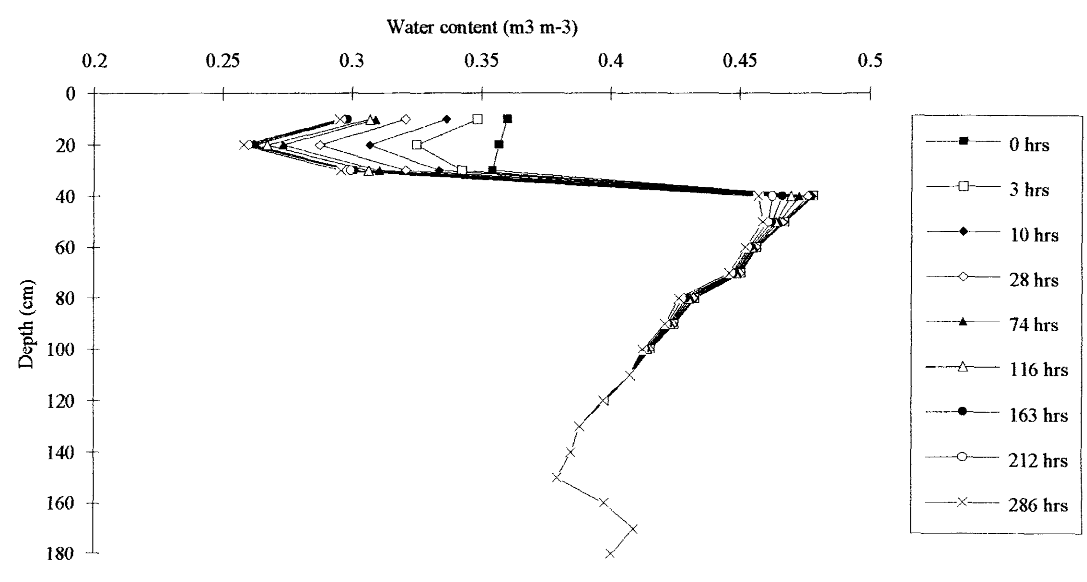

Figure 7.5: Change in profile water content with time

7.3.1.2 Change in matric potential over time

Figure 7.6 shows the change in matric potential over time for different depths. There is a gradual decrease in potential over time. Given that the 180 cm depth remains saturated throughout the 286 hours, as indicated by positive matric potentials (pressure potentials), and the matric potential at the 140 cm depth did not fall below -1 kPa, these two depths were excluded from the drainage evaluation as there were insufficient data points to test the model. It should be noted that the highest value possible for matric potential according to convention is zero (Hanks, 1992). A matric potential of zero means the soil is saturated. Once a soil is saturated, it becomes subjected to a positive pressure potential. Therefore, matric and pressure potentials are mutually exclusive.

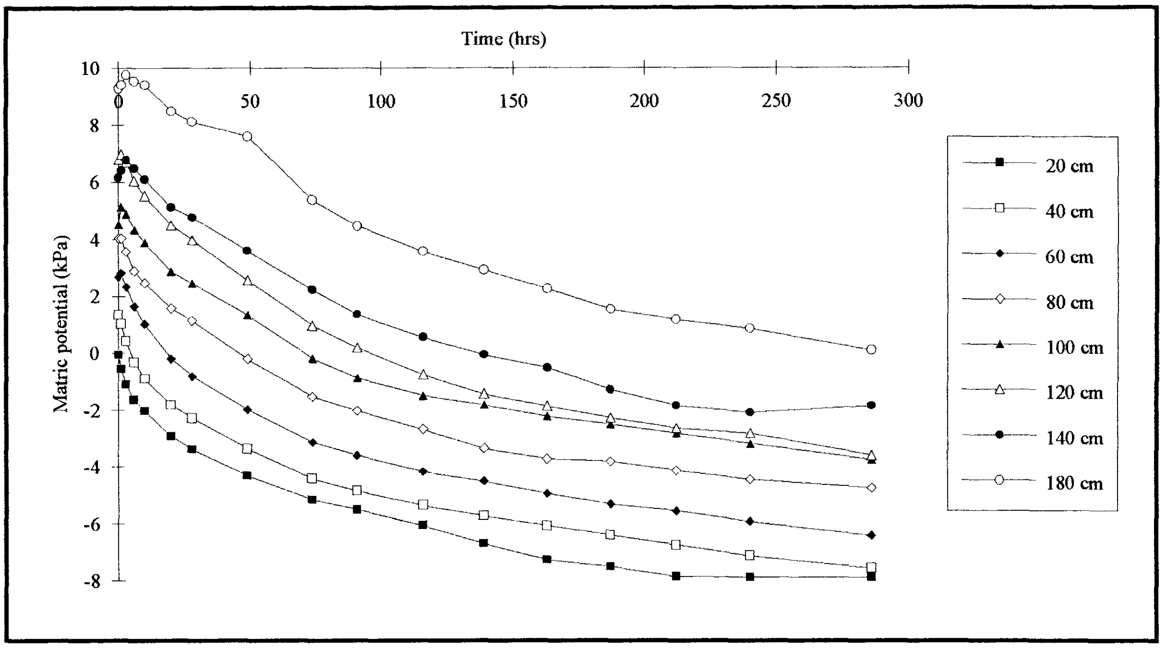

Figure 7.6: Changes in matric potential over time

Over the 286 hours there was only a small change in matric potential at each depth. The lowest matric potential of -7.9 kPa was recorded at the 20 cm depth. This small change in matric potential corresponds to the slow drying out of the drainage plot as indicated by the profile water contents in Figure 7.5.

7.3.1.3 Moisture characteristic measured in situ

Moisture characteristics for each depth for which it was possible to derive relationships from field data are given in Figure 7.7. The *in situ* data points used for determining the water retention relationships are tabulated in Appendix 1.1.

The *in situ* moisture characteristics are very steep, particularly at the 40 cm depth and below. The range of matric potentials measured is very narrow and the subsequent change in water content is very small. As discussed in Section 7.2.2.2, there is not a wide enough range of soil water content and matric potential for Campbell's (1974) water release function to give a sensible fit. Therefore, a combination of laboratory and *in situ* moisture characteristic points were used for the SWIM initialisation.

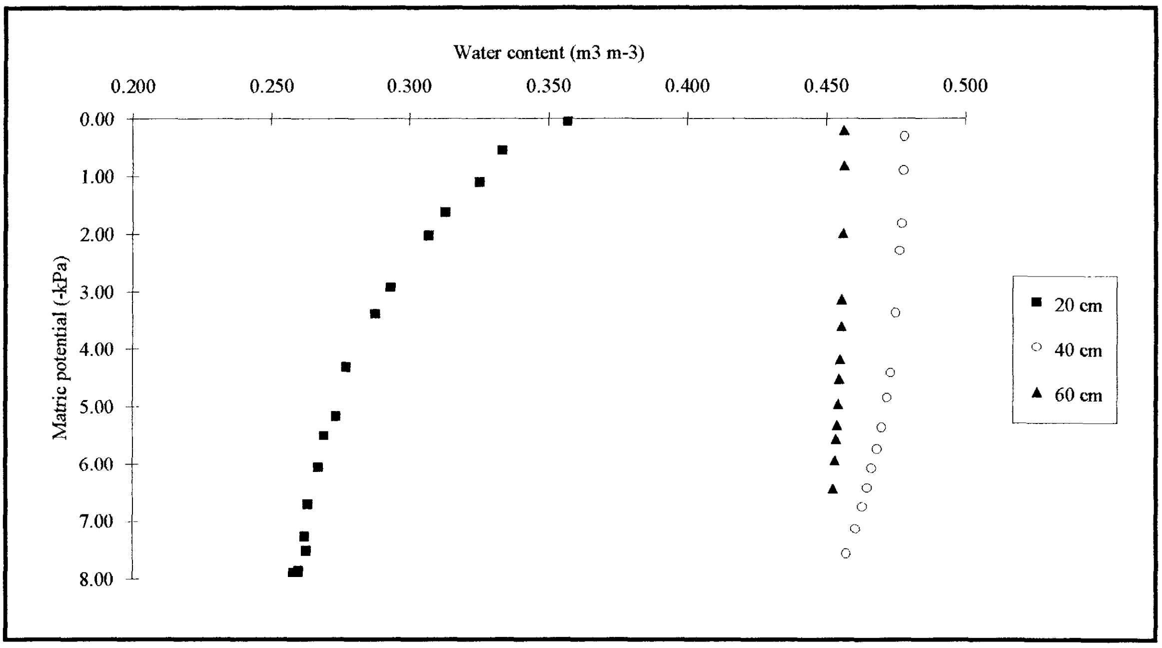

a) 20, 40 and 60 cm depths

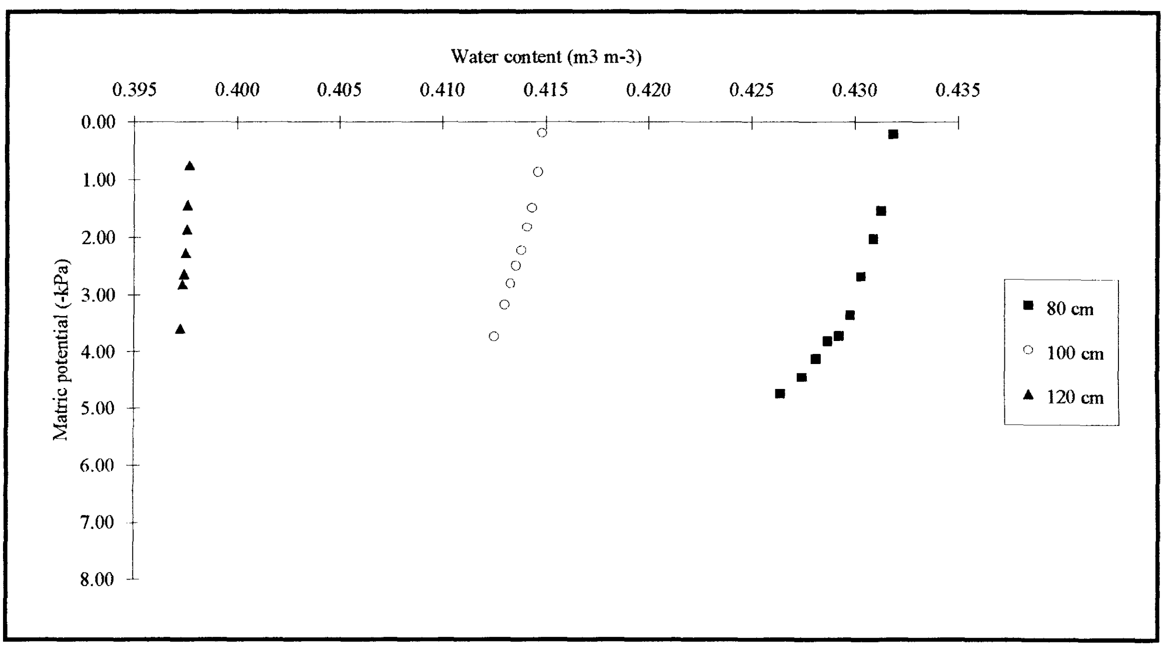

b) 80, 100 and 120 cm depths

Figure 7.7: *In situ* moisture characteristics at selected depths

7.3.1.4 Moisture characteristic for SWIM initialisation

The combined laboratory and *in situ* moisture characteristic data for the A2 (20 cm), B1 (40 cm) and B2 (70 cm) horizons were fitted to Campbell's (1974) water release curve (Figure 7.8). The parameter values derived from the regression are given in Table 7.2. The coefficient of determination (R^2) value for the 20 cm depth is 0.90, whereas the R^2 for the B1 and B2 horizons are 0.98 and 0.96 respectively indicating a better fit by Campbell's (1974) function. Given that the A2 moisture characteristic data based only on laboratory data had a R^2 value of 0.99 (Section 6.3.1) and when the *in situ* moisture characteristic points at 20 cm depth are added the R^2 value drops, the *in situ* points do not correspond very well to the laboratory data. However, it was necessary to use the laboratory points so as to provide some dry end points for the *in situ* data. Most of the *in situ* matric potential data were close to air-entry potential so that a reliable estimate of b could not be obtained. The *in situ* points can be compared to the laboratory points at each depth in Figure 7.8.

Table 7.2: Parameters required for calculating Campbell's water release curve: *A* and *B* = regression coefficients, R^2 = coefficient of determination, θ_s = saturated water content, *b* = the slope of the moisture characteristic, and ψ_e = air-entry potential- Combined laboratory and *in situ* moisture characteristic for SWIM initialisation

	A2 (20 cm)	B1 (40 cm)	B2 (70 cm)
A	4.033	4.177	4.226
B	-0.139	-0.075	-0.085
R^2	0.896	0.978	0.961
θs (m3 m^{-3})	0.357	0.518	0.498
b	7.19	13.36	11.81
ψe (cm water)	-27.04	-21.72	-42.69

The moisture characteristic curves are much steeper for the B horizons as indicated by the higher *b* values compared to the 20 cm depth. As discussed in Section 6.3.1, the gleyed podzolic soil has a medium to heavy clay B horizon, which is capable of holding more water than the sandy clay loam A2 horizon, over a range of potentials. A high *b* value means a narrow pore size distribution, with a large change in potential required for a significant change in soil water content.

As the mean pore diameter becomes smaller the air-entry potential decreases, i.e. it becomes more negative (Campbell, 1985). This is supported by the low air-entry potential value of -42.69 cm H_2O for the medium to heavy clay textured B2 horizon. According to Schafer (1980), the clay content of the gleyed podzolic soil increases from 19.4 per cent in the 15-30 cm layer to 59.4 per cent in the 30-51 cm layer to a maximum clay percentage of 65.4 in the 76-91 cm layer . Therefore, the B1 horizon would have been expected to have a lower air-entry value than the lighter textured A2 horizon. The air-entry potential calculated for the A2 horizon is probably not as representative of field values as the B1 and B2 air-entry values because of the differences between *in situ* and laboratory moisture characteristic data as previously discussed.

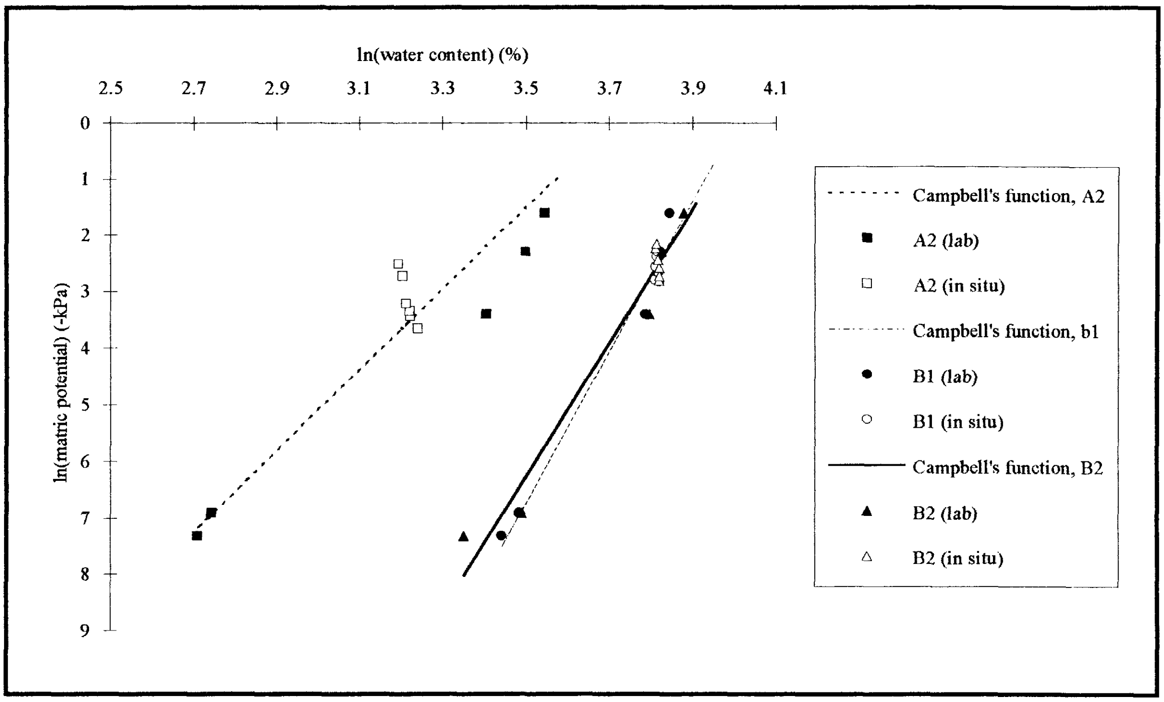

Figure 7.8: Combined laboratory and *in situ* moisture characteristic for the A2 (20 cm), B1 (40 cm) and B2 (70 cm) horizons

The new air-entry potentials at different depths (used for SWIM initialisation), based on their corresponding saturated water content measured *in situ* are presented in Table 7.3. The slope of the 40 cm moisture characteristic remains the same as the B1 (40 cm) moisture characteristic measured above (Table 7.2). Likewise, the slopes of the 60, 80, 100 and 120 cm moisture characteristics remain the same as the B2 (70 cm) moisture characteristic (Table 7.2).

Table 7.3: New air-entry potentials for selected depths based on saturated water content measured *in situ*

	Depth (cm)				
	40[a]	60[b]	80[b]	100[b]	120[b]
b	13.36	11.81	11.81	11.81	11.81
In situ θs (m3 m-3)	0.4784	0.4567	0.4330	0.4156	0.3980
ψe (cm H20)	-62.48	-119.17	-223.59	-362.64	-605.56

[a] Calculated from B1 (40 cm) moisture characteristic, [b] Calculated from B2 (70 cm) moisture characteristic

7.3.1.5 Hydraulic conductivity function measured in situ

The volume of water flowing per unit time per unit area, i.e. the soil water flux (q), was calculated and integrated over each depth and the data are presented in Table 7.4. The soil water flux is proportional to the hydraulic gradient, where the proportionality factor is hydraulic conductivity (K). The flux through each layer decreased over time due to a decrease in hydraulic conductivity with decreasing water content. The negative fluxes at the 20, 40 and 60 cm depths are a result of very small changes in water content over time so that the errors in NMM measurements result in apparent increases in moisture content at some recording times. The hydraulic gradients shown in Table 7.5 are all between zero and -1 indicating downward water movement due to both gravitational and matric forces. All data used to calculate the soil water flux, hydraulic gradients and the $K(\theta)$ and $K(\psi)$ functions are tabulated in Appendices 1.2, 1.3 and 1.4.

Table 7.4: The volume of water flowing per unit time per unit area (soil water flux) integrated over depth

	Soil water flux (mm/hr)					
Time (hrs)	**20 cm**	**40 cm**	**60 cm**	**80 cm**	**100 cm**	**120 cm**
0-1	2.437	4.540	4.547	4.551	4.553	4.554
1-3	0.431	0.762	0.770	0.773	0.776	0.777
3-6	0.787	1.237	1.245	1.248	1.251	1.252
6-10	0.086	0.203	0.210	0.214	0.217	0.217
10-20	0.280	0.455	0.462	0.466	0.468	0.469
20-28	0.069	0.139	0.147	0.150	0.153	0.154
28-49	0.089	0.169	0.176	0.180	0.183	0.184
49-74	0.023	0.032	0.039	0.043	0.046	0.047
74-91	0.062	0.096	0.103	0.106	0.109	0.110
91-116	-0.018	-0.005	0.003	0.006	0.009	0.010
116-139	0.055	0.102	0.109	0.113	0.116	0.116
139-163	0.013	0.009	0.016	0.020	0.023	0.023
163-187	-0.005	-0.008	-0.001	0.003	0.005	0.006
187-212	0.020	0.041	0.048	0.052	0.055	0.055
212-240	0.013	0.028	0.035	0.039	0.042	0.043
240-286	-0.002	0.005	0.013	0.016	0.019	0.020

Table 7.5: The change in hydraulic gradient over time

	Hydraulic gradient (I)				
Time (hrs)	**40 cm**	**60 cm**	**80 cm**	**100 cm**	**120 cm**
0-1	-0.220	-0.275	-0.471	-0.275	-0.629
1-3	-0.134	-0.216	-0.377	-0.228	-0.597
3-6	-0.145	-0.189	-0.330	-0.200	-0.487
6-10	-0.192	-0.161	-0.291	-0.208	-0.448
10-20	-0.263	-0.137	-0.240	-0.236	-0.436
20-28	-0.326	-0.130	-0.189	-0.263	-0.420
28-49	-0.377	-0.161	-0.157	-0.283	-0.416
49-74	-0.444	-0.232	-0.200	-0.326	-0.405
74-91	-0.495	-0.275	-0.279	-0.397	-0.409
91-116	-0.515	-0.299	-0.310	-0.471	-0.456
116-139	-0.479	-0.354	-0.314	-0.511	-0.515
139-163	-0.424	-0.397	-0.310	-0.519	-0.558
163-187	-0.424	-0.369	-0.295	-0.566	-0.629
187-212	-0.428	-0.334	-0.291	-0.613	-0.723
212-240	-0.460	-0.322	-0.299	-0.605	-0.738
240-286	-0.566	-0.299	-0.306	-0.648	-0.621

The hydraulic conductivity function is shown in relation to water content in Figure 7.9 and to matric potential in Figure 7.10. The $K(\theta)$ and $K(\psi)$ functions vary with depth because of the differences in soil physical properties, especially texture and porosity. The erratic nature of the curves is due to the small errors in water content measurement which are translated into K error. The $K(\theta)$ functions at each depth are steep at moisture contents close to saturation, with a small loss in water content resulting in a large decrease in hydraulic conductivity. However, once the soil dries to a certain water content at each depth, further changes in K are very small. Given that a less than 1 per cent change in water content has a large effect on K, accurate measurement of water content is particularly important for reliable $K(\theta)$ functions.

Similar results were found for other duplex soils by Rose *et al.* (1965), Olsson and Rose (1978), and Rab *et al.* (1987). Olsson and Rose (1978) measured $K(\theta)$ *in situ* at several depths for a red-brown earth and found that as clay content increased, greater water contents were required for the same hydraulic conductivity. The predominance of clay particles (<0.002 mm) and thus micropores in the gleyed podzolic subsoil results in low K values. These small pores require greater pressures before water will drain and therefore remain water-filled over a range of water contents and potentials (Olsson and Rose, 1978).

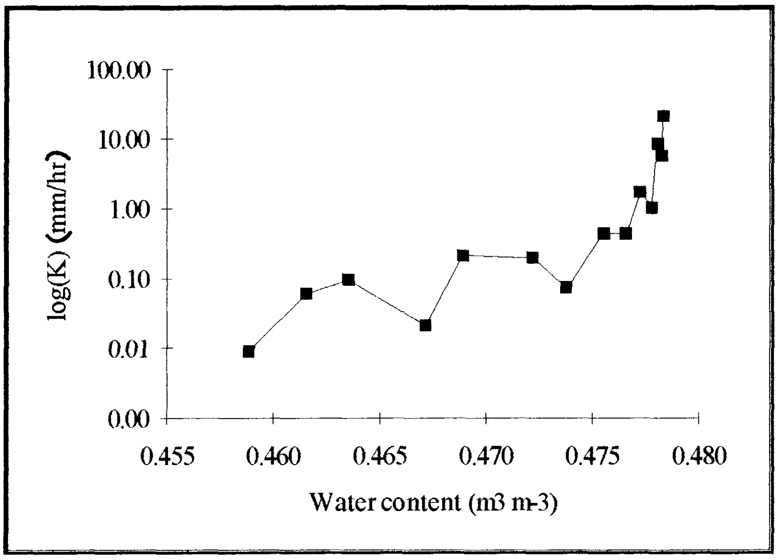

(a) 40 cm depth

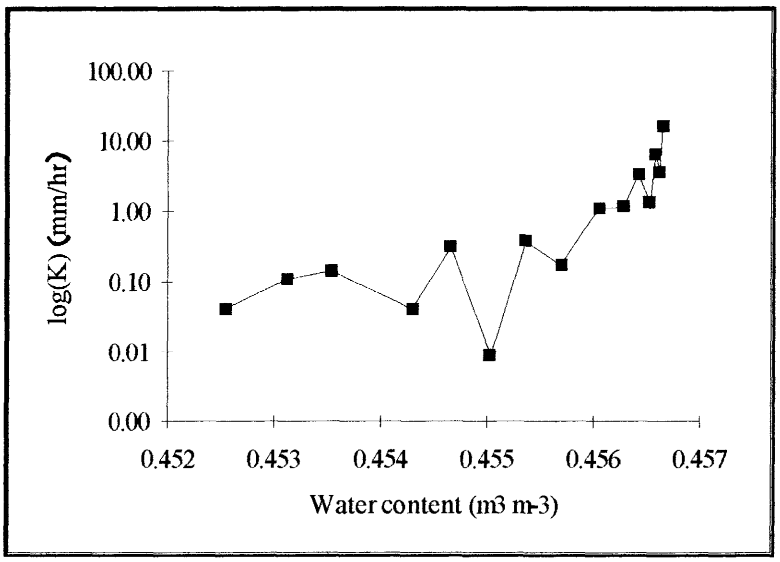

(b) 60 cm depth

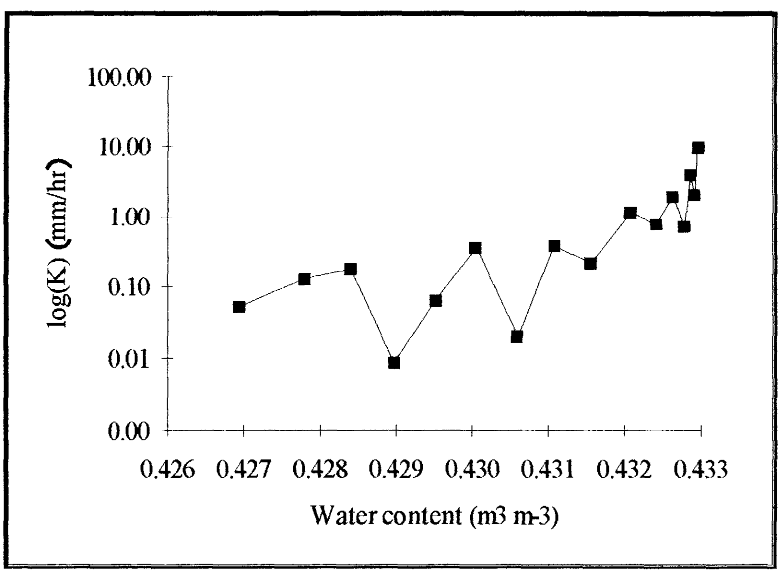

(c) 80 cm depth

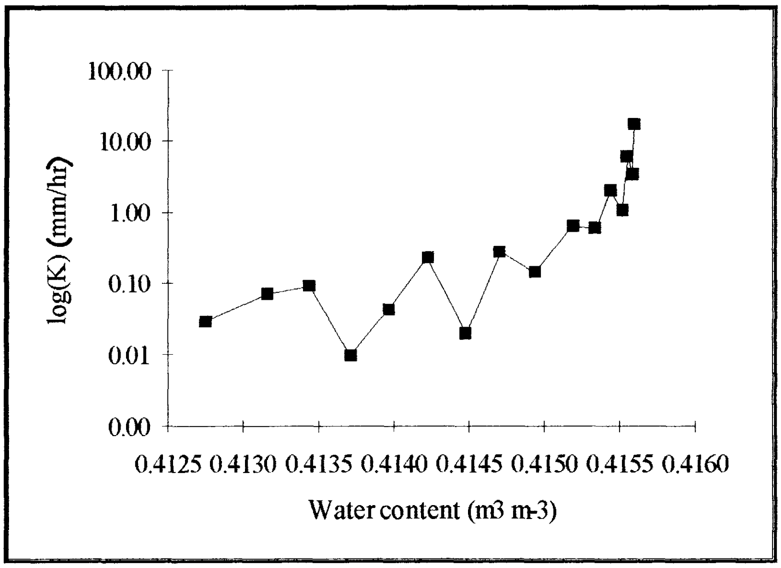

(d) 100 cm depth

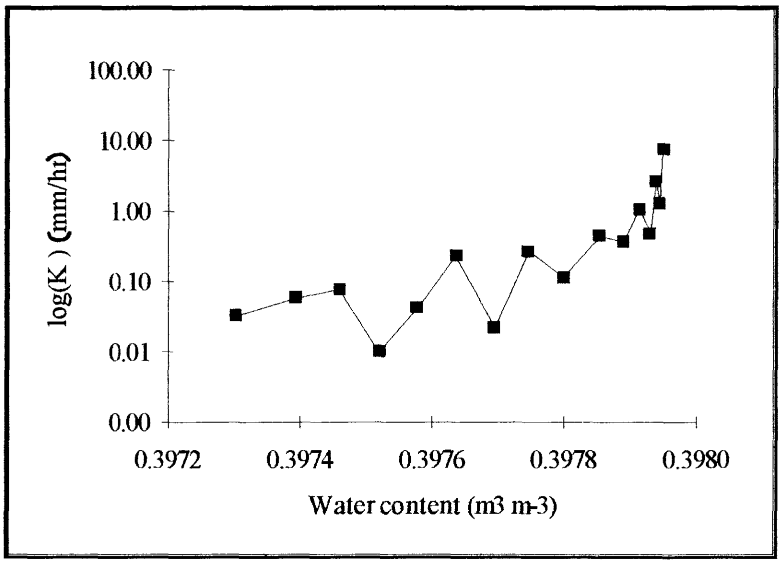

(e) 120 cm depth

Figure 7.9: K(θ) relationship from *in situ* measurements at selected depths

The K(ψ) functions presented in Figure 7.10 show a similar pattern to the K(θ) functions with hydraulic conductivity initially decreasing rapidly with decreasing matric potential. The curves for the 40 and 60 cm depths are steep at the wet end, indicating that a small change in potential will lead to a large change in conductivity. Once matric potential decreases below -10 cm H_2O (-1 kPa) the change in conductivity is relatively small. The hydraulic conductivities at 80, 100 and 120 cm depths are very low, and although the data is more erratic than for the shallower depths, there is still a marked decline in hydraulic conductivity with decreasing potential. K decreases much more quickly with decreasing matric potential for a light textured soil than for a heavier textured soil

(Williams, 1983). This is because of the large number of macropores, which hold more water and drain more easily, than the micropores, which are predominant in heavier textured clay soils.

These differences in hydraulic conductivity with depth affect water uptake by plant roots. Olsson and Rose (1978) suggest that the predominance of fine pores in the subsoil of a duplex soil contributes to the steep moisture characteristics, high water contents at low potentials (1500 kPa) and low amounts of available water. The consequent low macroporosity of the subsoil also contributes to other practical problems such as prolonged wet periods after rainfall or irrigation, thus poor aeration, making conditions unfavourable for plant growth and soil biological activity.

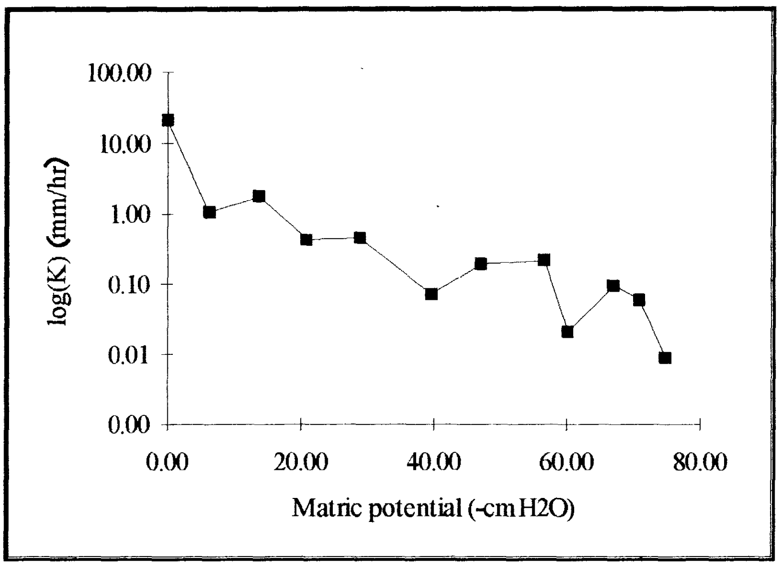

(a) 40 cm depth

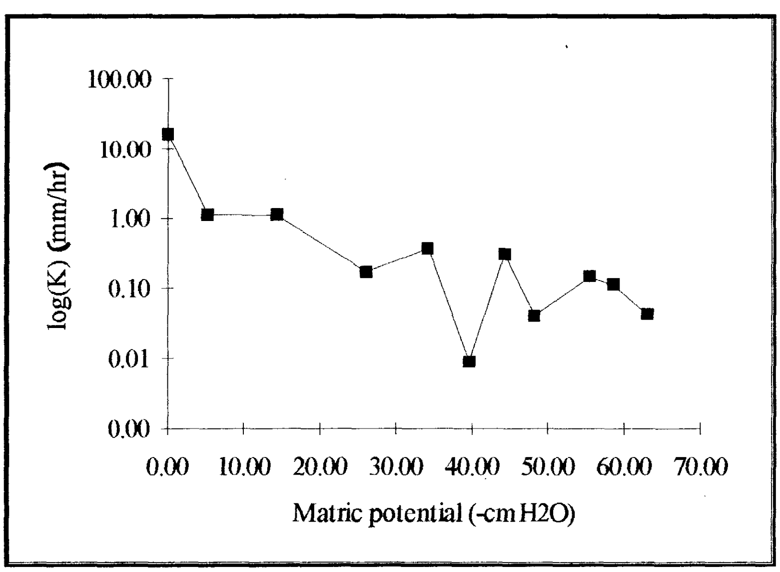

(b) 60 cm depth

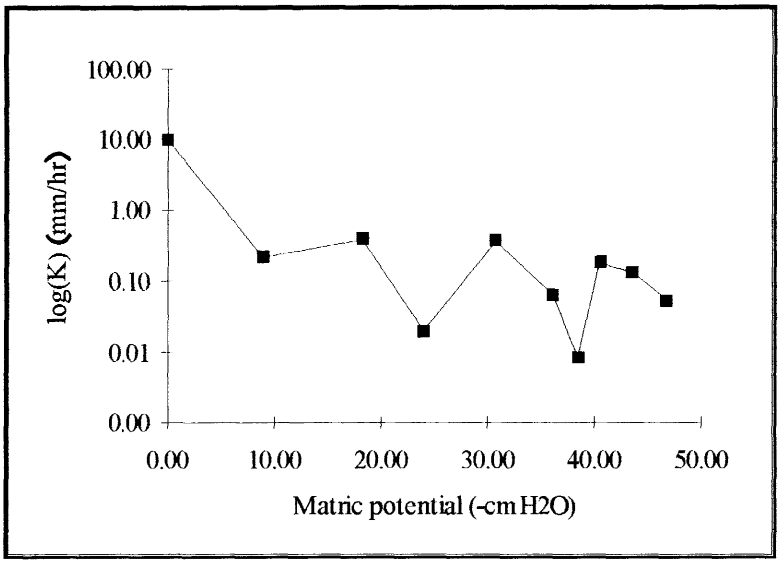

(c) 80 cm depth

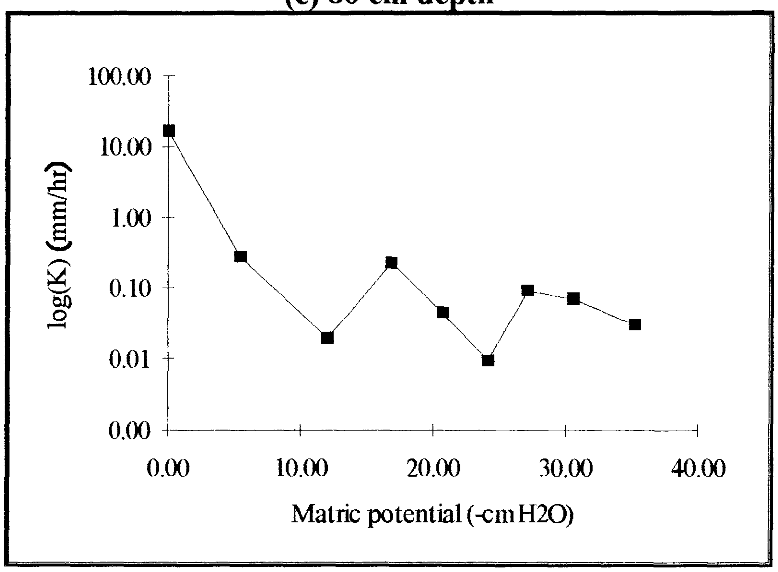

(d) 100 cm depth

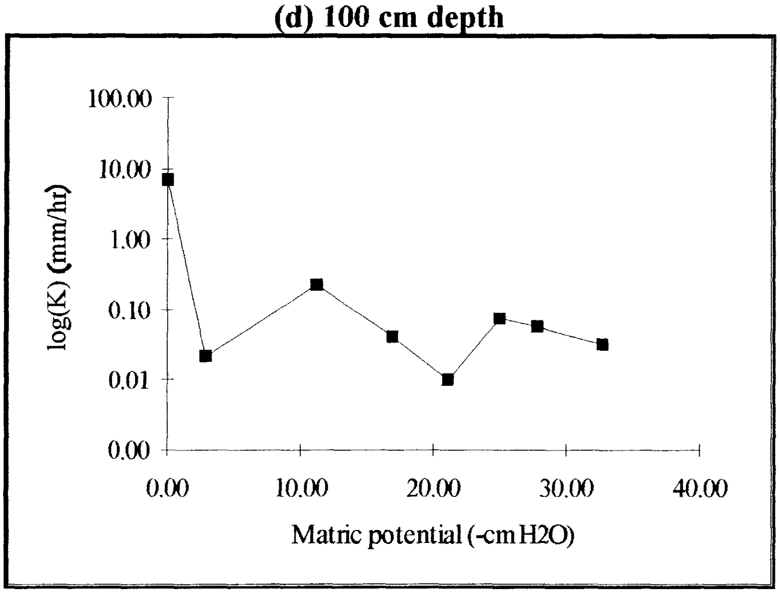

(e) 120 cm depth

Figure 7.10: K(ψ) relationships from *in situ* measurements at selected depths

7.3.1.6 Hydraulic conductivity function determined from moisture characteristic data

The hydraulic conductivity function (K(θ)) was predicted from the combined laboratory and *in situ* moisture characteristic data (Section 7.2.2.2) using Campbell's (1974) equation. The parameters required to calculate Campbell's K(θ) function are given in Table 7.6. Since the slope of the moisture characteristic (*b*) was used to calculate the *m* value, accurate calculation of the *b* value is essential for reliable predictions of K(θ) using Campbell's (1974) equation (Section 7.2.1.7). Accurate calculation of the air-entry potential is also important.

Table 7.6: Parameters required for calculating Campbell's (1974) hydraulic conductivity function: K_S = saturated hydraulic conductivity, θ_S = saturated water content, *b* = the slope of the moisture characteristic, and *m* = 2*b*+3

Depth (cm)	Ks (mm hr^{-1})	θs (m3 m^{-3})	*b*	*m*
40	20.64	0.4784	13.36	29.72
60	16.54	0.4567	11.81	26.63
80	9.65	0.4330	11.81	26.63
100	16.54	0.4156	11.81	26.63
120	7.25	0.3980	11.81	26.23

From Figure 7.11 it is clear that the predicted and measured K(θ) functions do not match each other. The slope of the predicted K(θ) function is much smaller than the measured function. Again the problems previously met when fitting Campbell's (1974) water retention function to *in situ* moisture characteristic data arise. K = K_S from a matric potential of zero to the air-entry potential. Therefore, Campbell's (1974) K(θ) function does not give a good description of the field measured K(θ) function because it has a 'corner'. A smooth curve is a better description of the behaviour of field measured K data.

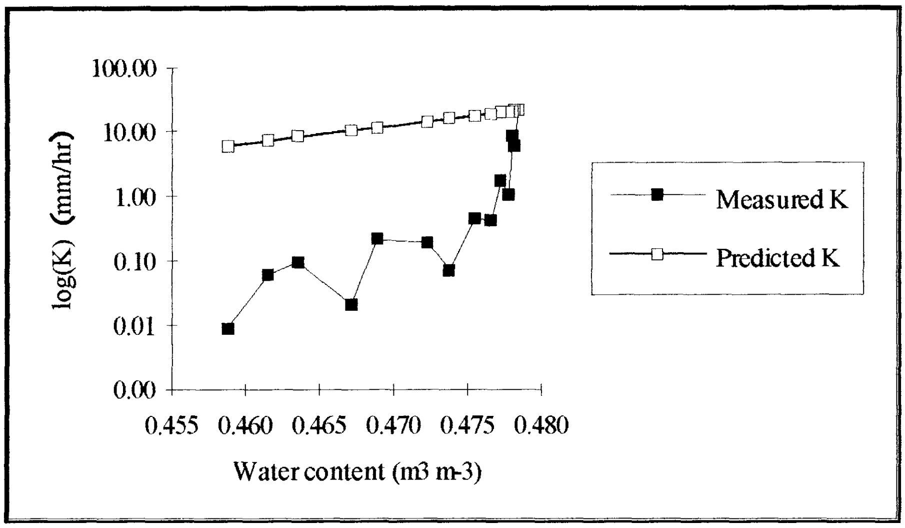

(a) 40 cm depth

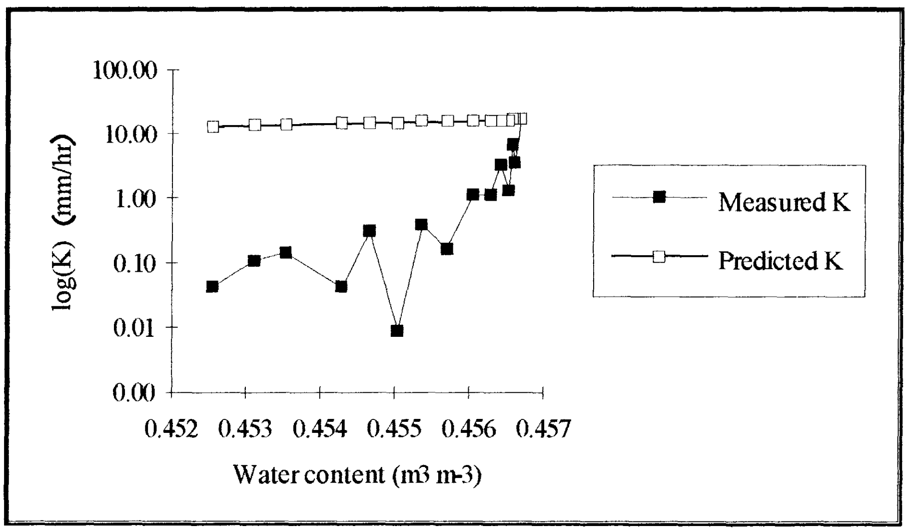

(b) 60 cm depth

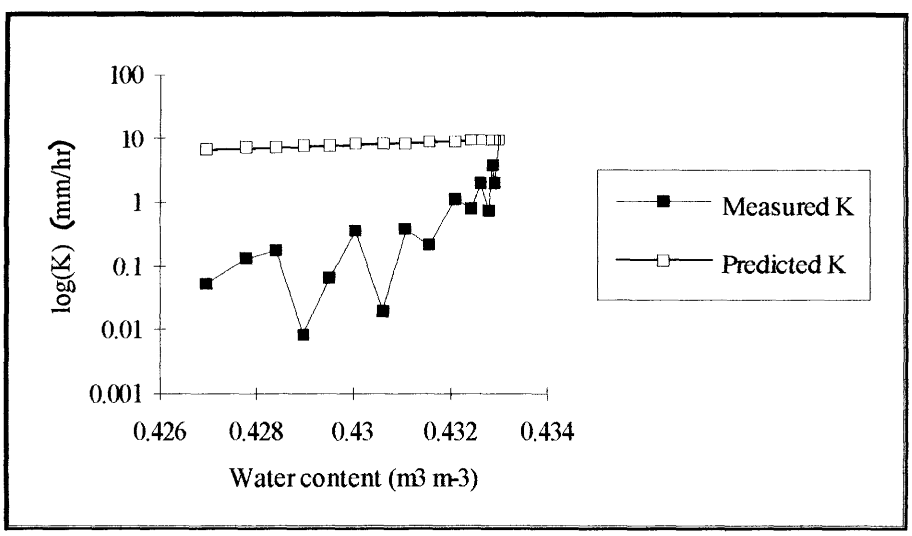

(c) 80 cm depth

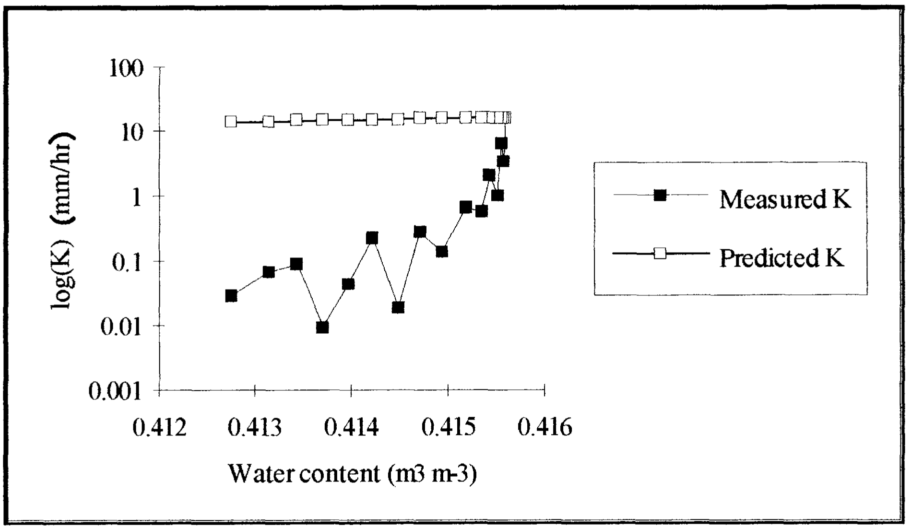

(d) 100 cm depth

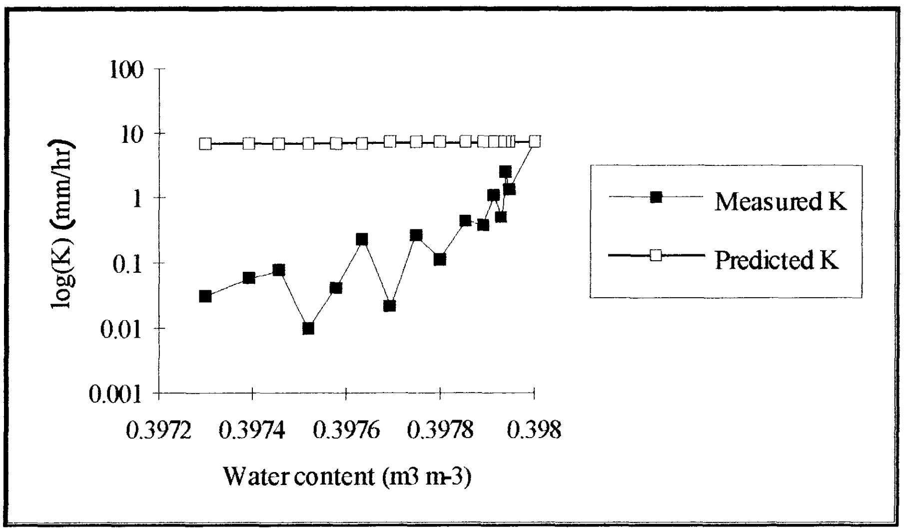

(e) 120 cm depth

Figure 7.11: The Campbell's (1974) K(θ) function predicted from water retention data versus the *in situ* K(θ) function at selected depths

7.3.1.7 Hydraulic conductivity function for SWIM initialisation

A better description of the field K(θ) function is required to initialise SWIM for the drainage evaluation. By incorporating two components into Campbell's (1974) K(θ) function as shown in Figure 7.4 a better match is obtained between the predicted and *in situ* K(θ) functions (Figure 7.12). This modification allows the slope of the function to change as water content decreases. At high water contents the slope is very steep, but once a certain water content is reached it flattens out. The parameters required to calculate the two-piece K(θ) function are shown in Table 7.7.

Table 7.7: Parameters required for calculating the modified two-piece Campbell's (1974) hydraulic conductivity function: θ_s = saturated water content, *b* = the slope of the moisture characteristic, $K_s = K_s + K_m$, and *n* and *m* are constants

Depth (cm)	θs (m3 m^{-3})	*b*	Ks (mm hr^{-1})	*n*	Km (mm hr^{-1})	*m*
40	0.4784	13.36	18.91	195	1.73	10
60	0.4567	11.81	15.23	520	1.30	31
80	0.4330	11.81	7.71	620	1.94	28
100	0.4156	11.81	15.52	1500	1.04	55
120	0.3980	11.81	6.76	950	0.49	130

Due to the erratic nature of the measured $K(\theta)$ functions a precise description of field data using the modified Campbell's (1974) function is not possible. However, the greatest difference between measured K and predicted K occurs when the soil is close to saturation and this difference is no more than 4 mm/hr. At all other water contents there is less than a 0.5 mm/hr difference between measured and predicted K.

For SWIM to accurately simulate water movement through the profile, it relies on an accurate description of the hydraulic properties using Campbell's (1974) equations. If Campbell's (1974) equations do not well describe the hydraulic functions then the simulated results will not match the measured results.

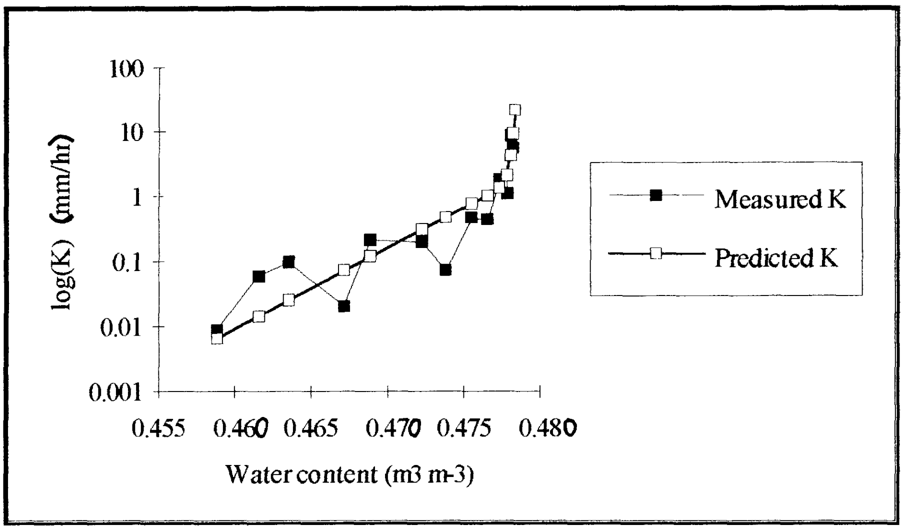

(a) 40 cm depth

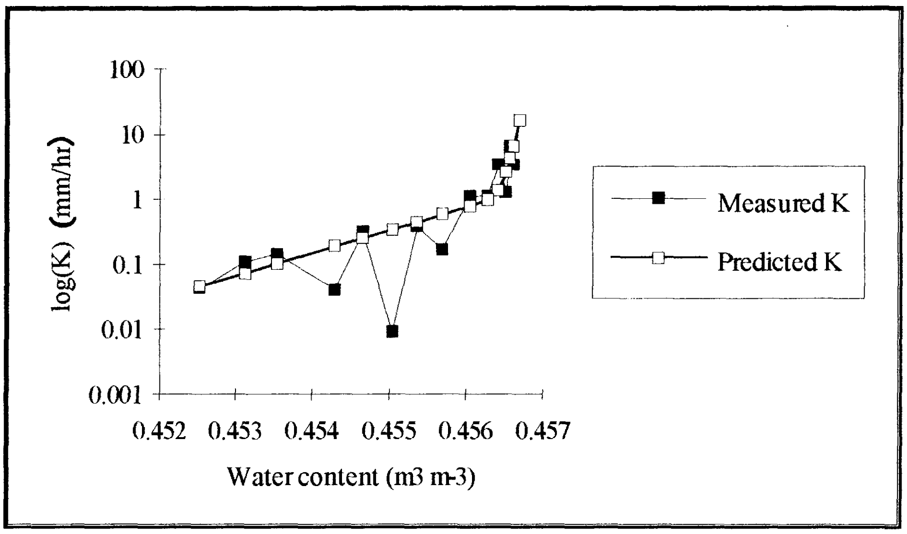

(b) 60 cm depth

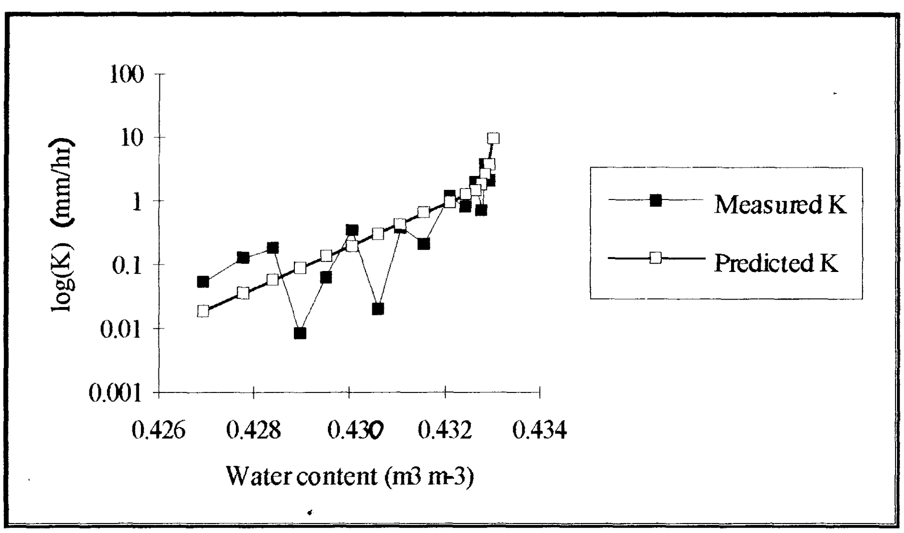

(c) 80 cm depth

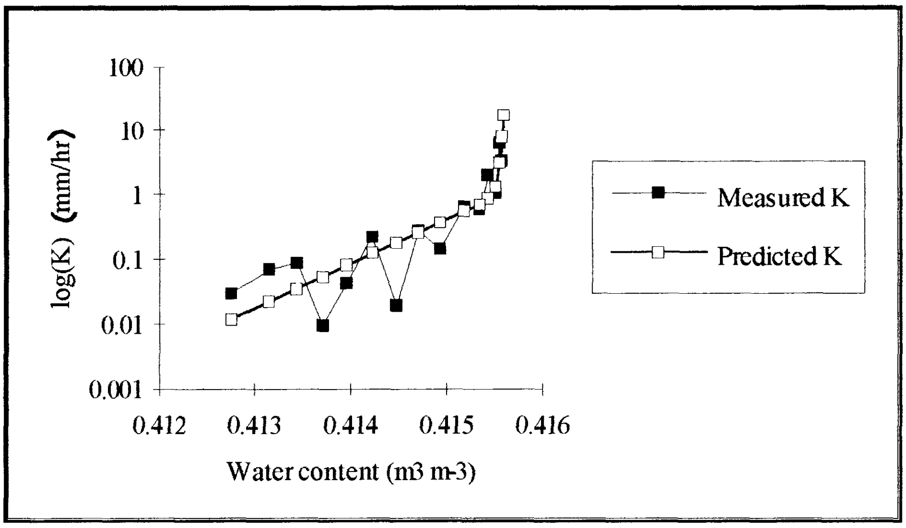

(d) 100 cm depth

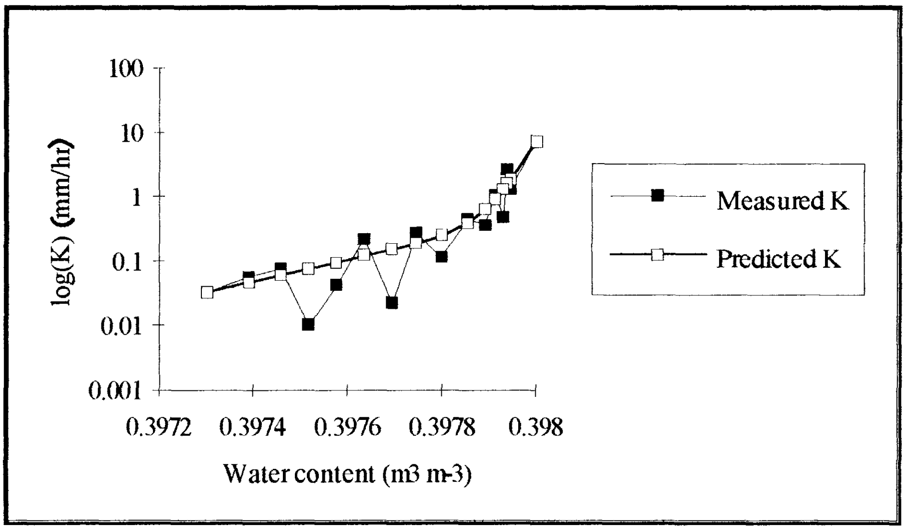

(e) 120 cm depth

Figure 7.12: The modified Campbell's (1974) K(θ) function predicted from water retention data versus the *in situ* K(θ) function at selected depths

7.3.1.8 Drainage

The amount of water draining from each soil layer increases rapidly up until the 50th hour but thereafter increases slowly particularly for the 20 cm depth (Figure 7.13). Redistribution of soil water throughout the profile is a result of both matric and gravitational forces. When the drainage plot was first saturated the hydraulic conductivity at each depth was at a maximum. Over time the redistribution of soil water slowed down for the following reasons: 1) hydraulic conductivity decreased with decreasing water content (Figures 7.9 and 7.10) and 2) the hydraulic gradients became smaller (weaker) as the soil moisture content becomes more uniform over depth (Table 7.5). With both hydraulic conductivity and hydraulic gradient decreasing simultaneously the soil water flux out of each layer also decreases (Table 7.4), which ultimately reduces the amount of drainage. The total amount of water which drained below the 120 cm depth was 30.7 mm over the 286 hour period.

Drainage through the profile is very slow, which is supported by the small change in profile water content, especially at depths greater than 40 cm, as shown in Figure 7.5. Water redistribution is important as is determines the amount of water retained at various times by different soil layers and therefore affects the amount of water available to plants. The rate and duration of downward water movement during redistribution determines the effective water storage capacity of the soil. The small amount of drainage water moving out of the soil profile suggests a high water holding capacity, but plant available water is probably reduced in the subsoil due to the predominance of fine pores. Loss of plant nutrients in drainage water would be also be minimal given the small amount of drainage.

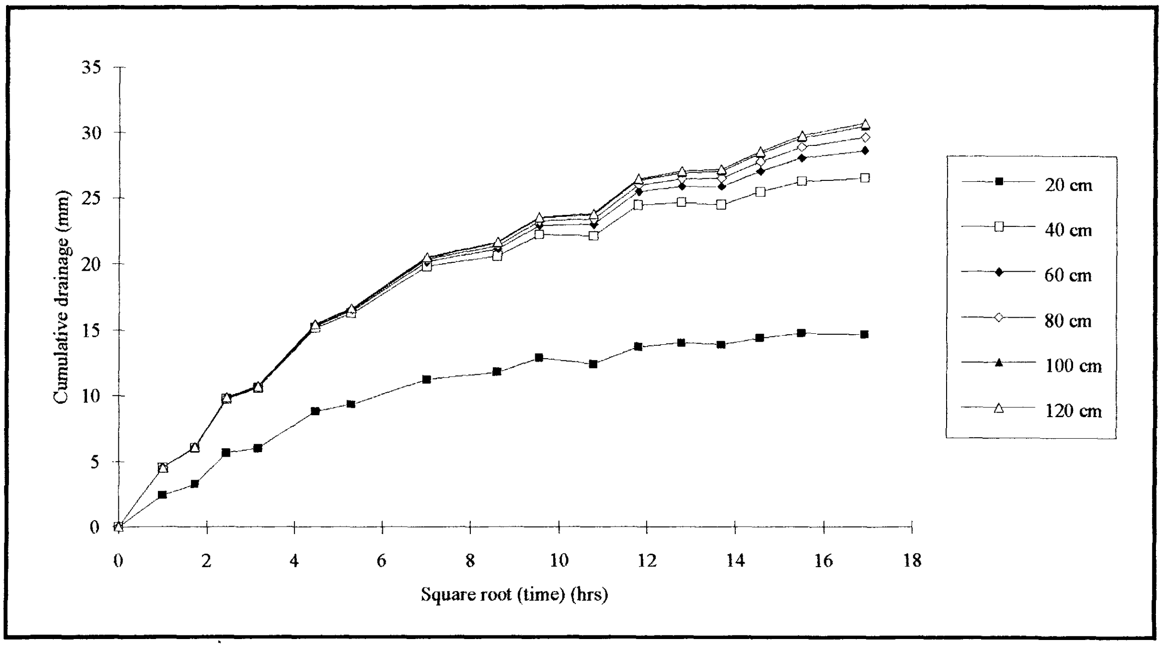

Figure 7.13: Cumulative drainage over time from various depths

7.3.2 Evaluation of the drainage component of SWIM

7.3.2.1 A comparison of measured and simulated water content at selected depths

The simulated and measured water content over time at selected depths are shown in Figure 7.14. The differences between simulated and measured values decrease with depth suggesting the model's inputs describe the subsoil more accurately. However, the change in water content over time decreases with depth and therefore the range of water contents over which to test the model differs between the depths.

The largest deviation between modelled and measured water content occurred at the 20 cm depth, despite the initial water content being the same. The differences between measured and predicted water contents at 20 cm depth increased with time, with predicted water content being 12 per cent higher than measured water content at 286 hours. The predicted moisture content did not decrease as the measured did, probably due to differences in the $K(\theta)$ functions.

There was a less than 2 per cent difference between measured and predicted water contents at 40 cm, and the differences were less than 1 per cent at 60, 80, 100 and 120 cm.

Redistribution of soil water depends on the hydraulic conductivity, which is a function of water content. For the 20 cm layer SWIM predicts the $K(\theta)$ function from the moisture characteristic data. An accurate calculation of the air-entry potential is critical for a good prediction of $K(\theta)$ since the hydraulic conductivity is equal to the saturated hydraulic conductivity right up until the air-entry potential is reached, as discussed in Section 7.3.1.6. Therefore, if the air-entry is higher than that measured, then the hydraulic conductivity will begin to decrease at higher potentials resulting in less water movement; likewise, if the actual air-entry potential is lower than the measured value, then the hydraulic conductivity will be higher over a larger range of potentials, resulting in more water movement. There was no measured $K(\theta)$ function for the 20 cm depth, and therefore no way of checking whether or not Campbell's (1974) $K(\theta)$ function was an accurate description of the field $K(\theta)$ function at this depth.

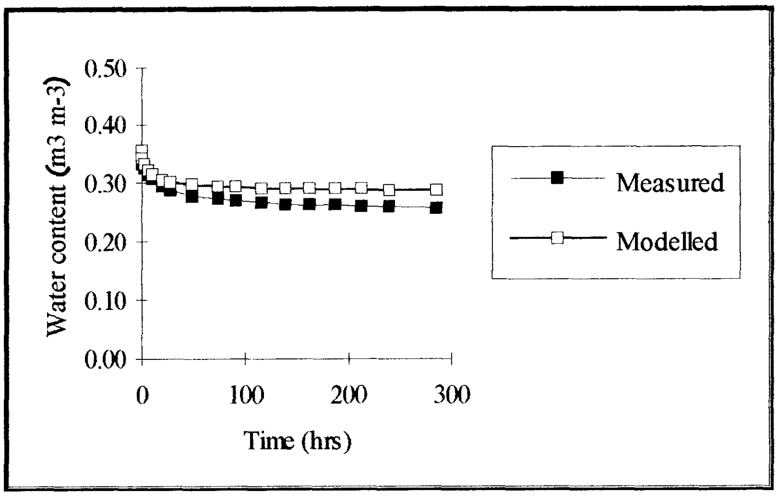

(a) 20 cm

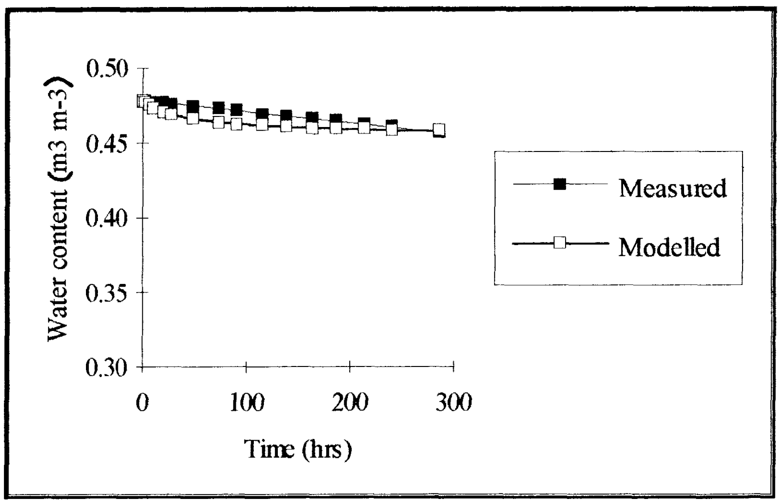

(b) 40 cm

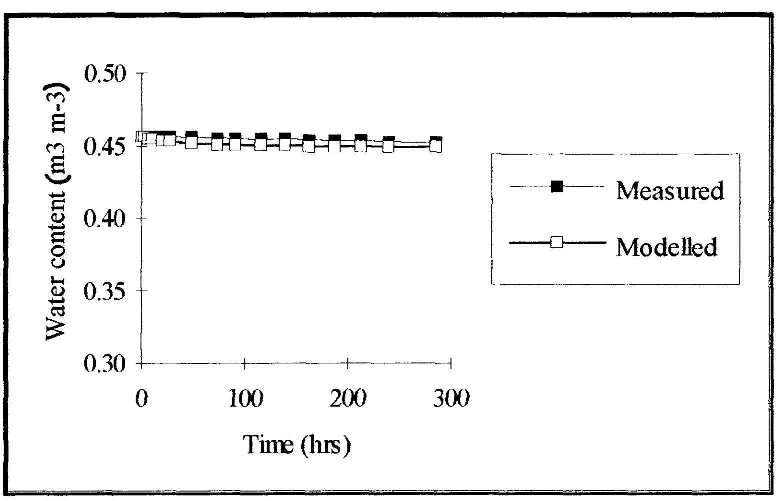

(c) 60 cm

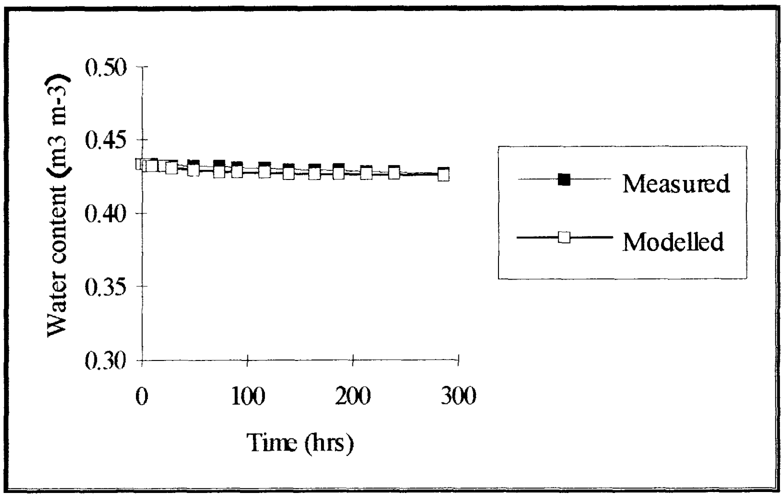

(d) 80 cm

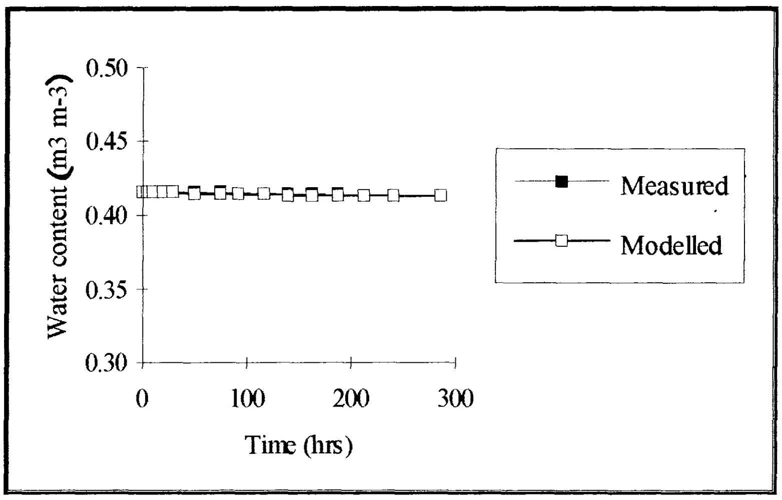

(e) 100 cm

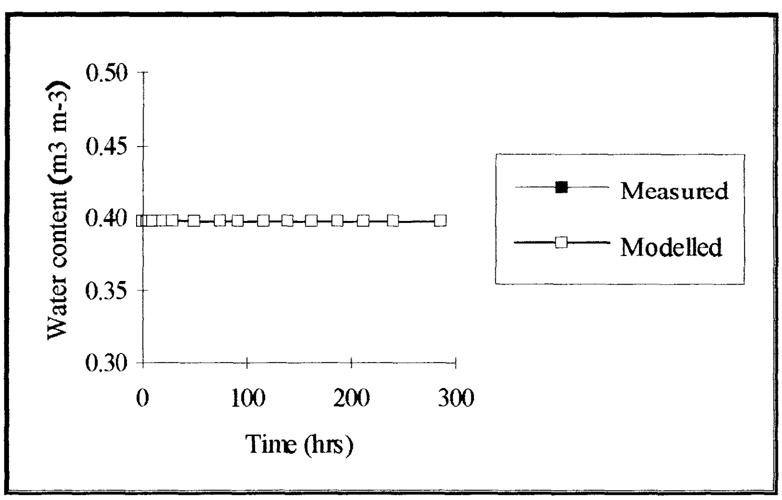

(f) 120 cm

Figure 7.14: A comparison of measured and SWIM predicted water content over time

7.3.2.2 A comparison of measured and simulated profile water contents

The measured and modelled soil water profiles are shown in Figure 7.15. At 0 hours the initial water content at 10 cm depth does not match the measured data. However, at this depth the accuracy of the measured water content is questionable as the neutron probe's 'sphere of influence' may extend above the soil surface. At the end of the simulation (286 hours) there is little difference between the modelled and measured water contents at depths below 30 cm. At the 20 cm depth there is an 11 per cent difference between modelled and measured water content. There is also a 4 per cent difference at 10 cm and a 3 per cent difference at 70 cm. At all other depths the difference is about 1 per cent or less. As a result of spatial variability of the soil there may be differences between the hydrological properties of the layers used in the model and those actually occurring in the field. For example, the hydraulic properties at the 70 cm depth are based on those measured at the 60 cm depth. If the 70 cm depth had its own set of hydraulic properties a more accurate simulation might have been obtained.

At the 20 cm depth, given the difficulty in determining the moisture characteristic at this depth (Section 7.2.2.2), the differences between the modelled and measured water content are attributed to the moisture characteristic not representing the field data accurately, rather than to the model not solving Richards' equation correctly. Error in moisture characteristic determination has resulted in error in the predicted $K(\theta)$ function used to initialise SWIM. Subsequently, the predicted drainage and redistribution pattern has not exactly matched the field observations.

There are several reasons why measured and predicted data differ. There could be error in Richards' equation solution (or any other calculations) in SWIM. The assumptions used in the simulations, such as assuming drainage below the 120 cm layer is due to gravity only, or the assumption that Campbell's (1974) equations describe the hydraulic input data, may be inappropriate. Since the differences between predicted and modelled data are relatively small, the error is more likely to be due to error in the measurement of hydraulic properties. This error could be a result of spatial variation in data used from outside the drainage plot or from spatial variation within the drainage plot, temperature gradients within the drainage plot, direct measurement error in either the field or laboratory techniques or from the assumptions used in the drainage plot calculations such as no evaporation.

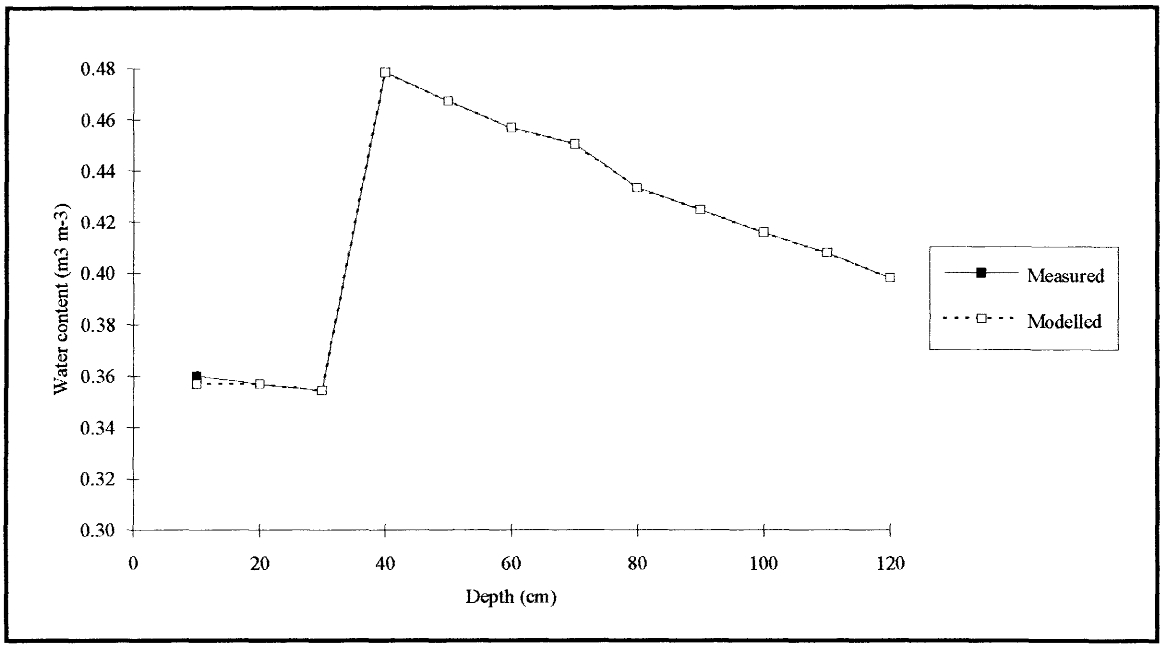

(a) 0 hours*

***Measured and modelled water content profiles coincide for the 20 to 120 cm depths**

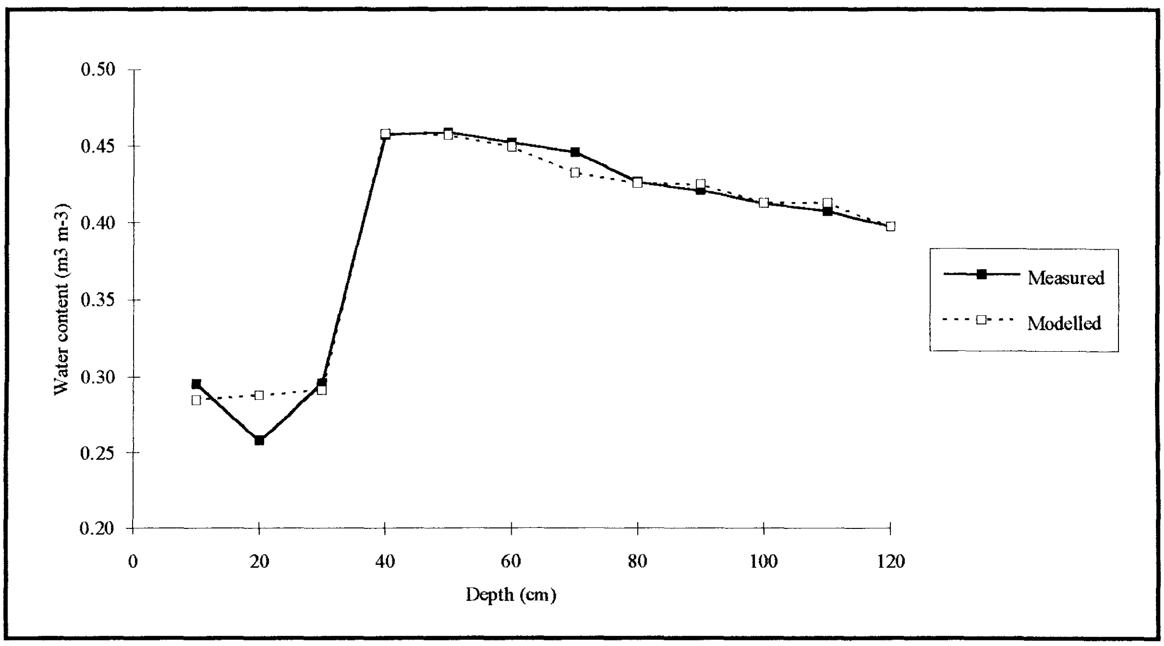

(b) 286 hours

Figure 7.15: A comparison of measured and SWIM predicted profile water contents at a) the start of the experiment and at (b) 286 hours

7.3.2.3 A comparison of measured and simulated drainage

The modelled and measured cumulative drainage from the 120 cm depth are presented in Figure 7.16. There is less than 2 mm difference between the measured and modelled drainage at all times up to 240 hours. At 286 hours the difference is only 3 mm. The amount of drainage depends on the maximum amount of water the soil profile can hold at saturation and how easily the water moves through the profile, i.e. the hydraulic conductivity. Differences between measured and modelled drainage are determined by the accuracy of the moisture characteristic and hydraulic conductivity function at each depth. Differences of 2-3 mm are very small and these results suggest that SWIM solves Richards' equation accurately to produce reasonable estimates of drainage from the gleyed podzolic soil.

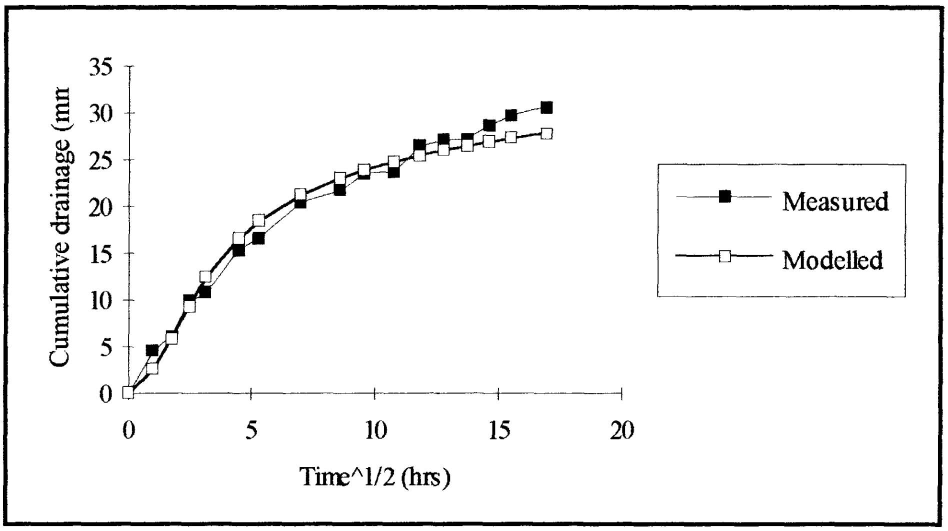

Figure 7.16: A comparison of measured and SWIM predicted drainage over time

7.3.2.4 Drainage over a 3000 hour simulation run

Using the inputs listed in Table 7.1 the SWIM simulation was run for 3000 hours (approximately 4 months) to examine the soil moisture profile over an extended time period. Figure 7.17 shows that between 286 and 3000 hours only a further 4.7 mm of water drained beneath the 120 cm layer. The change in profile water content between 286 and 3000 hours is shown in Figure 7.18. There is a less than a 3 per cent decrease in water content in the 0 to 30 cm layer and less than 1.5 per cent decrease at lower depths. This is due to the soil profile having dried down sufficiently to the point where the hydraulic conductivity is low, so that little water movement occurred. The largest fluxes occurred at saturation, and given the steep K(θ) functions (Figure 6.10) there is a rapid decline in K with decreasing water content. Therefore, the gleyed podzolic, which has no plants growing in it to remove water by transpiration, is likely to continue to drain extremely slowly over many months.

The practical implication of these results is that very little water is lost by drainage from this soil and therefore nutrient loss in drainage water would be minimal. In this simulation SWIM describes water movement through a soil profile with no vegetation. In a pasture or cropping soil there would probably be less drainage, but the profile would dry out much more rapidly due to water uptake by the plant. As water movement is slow through this soil, plant roots have ample time to absorb the available soil water and take up nutrients before they move out of the root zone. Slow drainage may also have some deleterious effects such as waterlogging and saturated excess runoff (Chapter 8, Section 8.3.1).

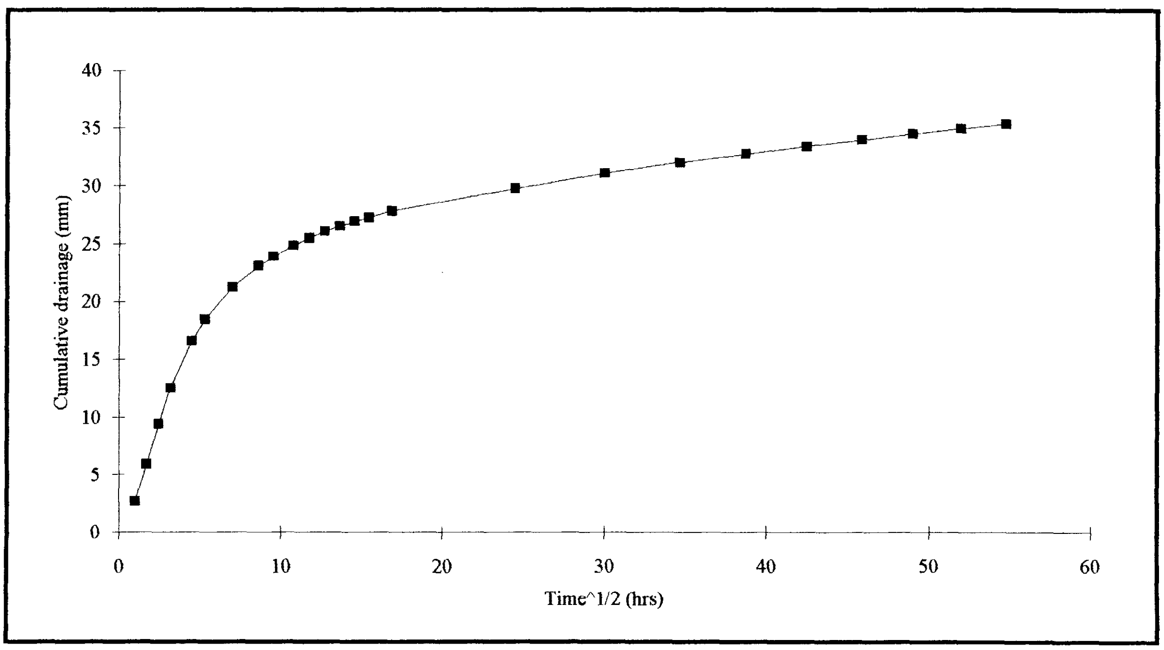

Figure 7.17: Cumulative predicted drainage over 3000 hours (approximately 4 months)

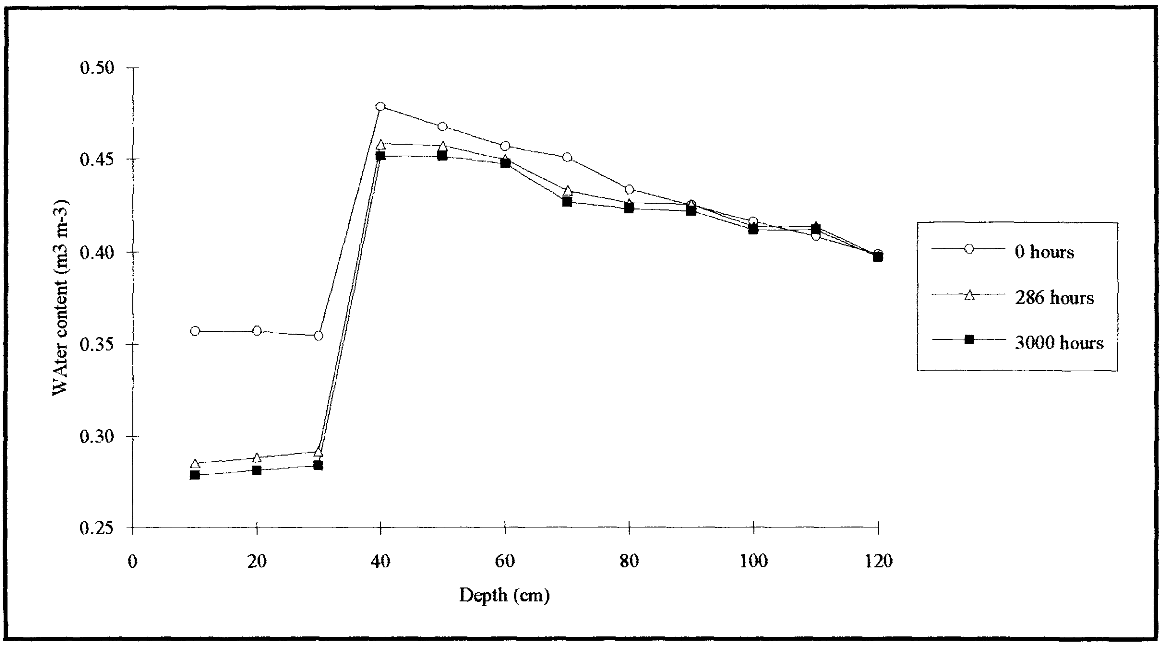

Figure 7.18: Changes in predicted profile water content over 3000 hours (approximately 4 months)

7.3.2.5 Sensitivity analysis

The sensitivity of the SWIM model's drainage prediction to changes in the soil input parameters is shown in Table 7.8. The sensitivity analysis indicates that the model's prediction of drainage is most sensitive to the saturated water content (θ_s) and b, the slope of the best fit line relating θ to ψ on a log-log scale. Although all of the soil inputs are used to solve Richards' equation, which describes one dimensional vertical water flow, some inputs have a greater influence on SWIM output than others. A change in θ_s, ψ_e or b result in a change to both the moisture characteristic and the K(θ) function.

Table 7.8: The sensitivity of the SWIM model's drainage component to a 10 per cent change in the models soil input parameters

Input[a]	Change in input	Cumulative drainage (mm)	% change from base value[a]	mm change from base value[b]
θs	+ 10 %	30.3	8.9	2.5
	- 10 %	25.3	9.0	2.5
ψe	+ 10 %	27.1	2.5	0.7
	- 10 %	28.3	1.8	0.5
b	+ 10 %	25.7	7.6	2.1
	- 10 %	30.3	9.0	2.5
Ks	+ 10 %	28.4	2.0	0.6
	- 10 %	27.8	0.2	0.0
Ks	+ 50 %	29.3	5.2	1.5
	- 50%	25.8	7.2	2.0

[a] θs is saturated water content, ψe the air-entry potential, b the slope of the best fit line relating θ to ψ on a log-log scale and Ks saturated hydraulic conductivity

[b] The base drainage value = 27.8 mm

A change in θ_S results in a parallel shift in the moisture characteristic, with the slope remaining the same. Therefore, an increase in θ_S causes a shift in the moisture characteristic such that more water is held at all potentials. This in turns means there is more water in the profile which may be lost through drainage. A decrease in θ_S results in less water being held at any given potential and thus less water available for drainage.

The b value describes the change in soil water content due to a change in matric potential. The smaller the slope, the greater the quantity of water that will drain as matric potential decreases. A 10 per cent decrease in b caused a 9 per cent increase in the amount of drainage predicted.

θ_S and b are also used in SWIM's prediction of the hydraulic conductivity function ($K(\theta)$) using Campbell's (1974) equation. An increase in θ_S or b causes a decrease in hydraulic conductivity at any given water content, whereas a decrease in θ_S or b results in an increase in hydraulic conductivity at any given water content. A change in the $K(\theta)$ function directly affects the amount of drainage as it affects the ease with which water moves through the soil profile.

A 10 per cent increase in saturated hydraulic conductivity (K_S) led to a less than 2 per cent change in cumulative drainage. However, the K_S of the subsoil is very low and therefore a change of 10 per cent in K_S means a change of less than 2 mm/hr. A 50 per cent change in K_S caused a 5 per cent increase in cumulative drainage. An increase in K_S leads to an increase in the hydraulic conductivity at a given water content resulting in greater water movement through the profile and more drainage.

The ability of SWIM to accurately predict drainage relies on the validity of the input data. The sensitivity analysis indicates that the model's drainage prediction is most sensitive to θ_S, b and K_S. Therefore, more care must go into their measurements for reliable estimates of drainage by SWIM.

7.4 Conclusion

The drainage plot was very slow to dry down. As a result the range of matric potentials and their corresponding water contents measured was narrow. The *in situ* moisture characteristics show that the B horizon holds more water over the range of potentials measured compared to the A horizon. This is due to the high clay content of the B horizon. The micropores in the clay B horizon hold onto water tightly requiring much lower potentials than the A horizon for water to drain. Therefore, hydraulic conductivity

(K) was lower in the B horizon compared to the A horizon. The greatest differences in K between depths occurred at the high water contents where small changes in water content had a large effect on K.

The hydraulic properties measured *in situ* in the gleyed podzolic soil suggest poor subsoil drainage. The total amount of water that drained below the 120 cm layer was 31 mm. However, the greatest amount of drainage occurred when the profile was saturated, with around 15 mm draining below the 120 cm depth within the first 24 hours. The small amount of drainage indicates that the gleyed podzolic has a high water holding capacity, however, plant available water is reduced in the subsoil due to the predominance of fine pores. The advantage of poor drainage is that there would only be a small loss of plant nutrients in drainage water. However, periods of waterlogging will adversely affect plant growth.

For SWIM to accurately simulate water movement through the soil profile, it relies on accurate descriptions of soil hydraulic properties using Campbell's (1974, 1985) water retention and hydraulic conductivity functions. In order to apply Campbell's water retention function to the *in situ* moisture characteristic data, laboratory determined moisture characteristic data was included. However, this resulted in some problems due to spatial variability, particularly at the 20 cm depth. The major source of variation was the depth to the B horizon.

Campbell's (1974) hydraulic conductivity function did not describe the field $K(\theta)$ function well. However, a modified Campbell's function, that accounts for initially high flows when the soil is close to saturation, provided a better description.

The prediction of soil water movement through the soil profile by SWIM agreed well with measured values. There was little difference between measured and predicted water content over time or the profile water contents. The largest deviation between predicted and measured values occurred at the 20 cm depth due to problems in applying Campbell's (1974) functions to data collected at this depth. The greatest difference between predicted and measured cumulative drainage at any time was 3 mm. The results indicate that the Richards' equation describes water movement through a gleyed podzolic well. However, model output is only as good as the inputs supplied, therefore accurate measurement of the moisture characteristic and hydraulic conductivity function are critical for reliable estimates of drainage by SWIM.

The sensitivity analysis found SWIM's drainage prediction to be most sensitive to changes in saturated water content and *b*. A change in either of these input parameters changes Campbell's (1974, 1985) water retention function and hydraulic conductivity function, therefore, changing the water redistribution and drainage pattern.

8.0 An application of SWIM to examine the effect of grazing on the soil water balance

8.1 Introduction

There is much evidence to suggest that the soil water balance is modified by grazing animals (Section 3.2.3). Trampling causes changes in soil surface hydraulic properties, thus changing the way in which water moves into and through the soil. Adverse effects by grazing on soil physical properties may result in decreased infiltration and increased runoff, which reduce the amount of water that is potentially available to plants (Alderfer and Robinson, 1947). Increased runoff also leads to an increase in soil erosion.

The principles governing water entry, storage and movement are derived from two important soil hydraulic properties: the moisture characteristic and the hydraulic conductivity function (Greacen and Williams, 1983). From Chapter 5 it is evident that the moisture characteristic and hydraulic conductivity of the surface layers differ between the grazed and ungrazed plots. It is to be expected that these differences would have an important effect on the soil water balance. The Soil Water Infiltration and Movement (SWIM) model can be used to examine the effects of grazing on the water balance. The output from the model will indicate changes to infiltration, water storage and deep percolation of water as affected by stocking rate.

Models may be used for improving the understanding of certain hydrological processes. They can be used to assess the effect of input parameters on a process and also provide estimates of actual quantities, as in the case of the SWIM model which quantifies the water balance. Water balance models have many beneficial applications. For example, previously measured soil data can be used to parameterise the model and simulations can be run with storms designed from historical weather data. This is much easier than trying to measure the water balance and waiting for large storms or a range of wet and dry days. However, a model's output will only be as good as the information supplied to it as inputs. There is generally some error associated with the determination of the inputs required by the model. A sensitivity analysis will determine the sensitivity of model output to uncertainty in input parameters (Cresswell *et al.*, 1994). Littleboy *et al.* (1992) suggested that a sensitivity analysis is required when obtaining values of input parameters by calibration, estimation or measurement. Obviously more care needs to be taken in selecting parameter values if a small change in that parameter causes a large change in the model's output.

The aim of this study is to examine the consequences of changed hydrological properties under grazing on the soil water balance as predicted by SWIM. Different simulations were run to examine the consequences of changes in rainfall intensity, initial matric potential and depressional storage on the soil water balance of an ungrazed and grazed site.

A sensitivity analysis was also carried out to determine the sensitivity of SWIM output to variation in the model's inputs.

8.2 Description of simulations

8.2.1 Initial input values

The inputs used to initialise SWIM are presented in Table 8.1.

Table 8.1: Inputs used for SWIM simulations: (a) soil hydraulic properties, (b) surface conductance data and (c) runoff data

(a): Soil hydraulic properties

(i): Zero graze

Layer	Depth cm	initial ψ cm H2O	θs $m^3\ m^{-3}$	ψe cm H2O	b	Ks $cm\ hr^{-1}$
Above compacted layer	0-18	-100	0.483	-22.02	4.22	21.48
Within compacted layer	18-24	-100	0.430	-17.10	4.81	5.32
Below compacted layer	24-36	-100	0.426	-7.87	5.92	3.68
B1	36-60	-100	0.518	-19.11	13.56	1.316
B2	60-100	-100	0.498	-46.97	11.56	0.225
B2	100-140	-100	0.498	-46.97	11.56	0.188
B2	140-150	-100	0.498	-46.97	11.56	0.05

(ii):10 DSE/ha

Layer	Depth cm	initial ψ cm H2O	θs $m^3\ m^{-3}$	ψe cm H2O	b	Ks $cm\ hr^{-1}$
Above compacted layer	0-18	-100	0.484	-15.44	5.039	7.19
Within compacted layer	18-24	-100	0.417	-16.20	5.764	8.62
Below compacted layer	24-36	-100	0.438	-14.72	7.778	3.46
B1	36-60	-100	0.518	-19.11	13.56	1.316
B2	60-100	-100	0.498	-46.97	11.56	0.225
B2	100-140	-100	0.498	-46.97	11.56	0.188
B2	140-150	-100	0.498	-46.97	11.56	0.05

(b): Surface conductance data

Parameter	Zero graze	10 DSE/ha
Initial soil surface conductance	43 /h	14 /h
Minimum soil surface conductance	43 /h	14 /h
Precipitation constant[a]	2.5 cm	2.5 cm
Effectiveness parameter[a]	0.184	0.184

(c): Runoff data

Parameter	Value
Initial soil surface storage[b]	0.2 cm
Minimum soil surface storage[b]	0.2 cm
Precipitation constant[a]	2.5 cm
Runoff rate factor[c]	2 and 50 (cm/h)/cm^p
Runoff rate power[c]	2
Initial surface water depth	0

[a] Ross (1990), [b] Moore and Larson (1979), [c] H. Cresswell *pers comm.*

The soil profile used in the simulations consisted of seven horizontally uniform layers, with hydraulic properties measured at defined intervals to a maximum depth of 150 cm. Although the gleyed podzolic has only five horizons (Table 4.2, Section 4.4), the soil was divided into a number of extra layers to allow for different hydraulic properties in the top 36 cm, as they are affected by grazing. As outlined in Section 2.3.2, water movement through the soil profile is governed by the soil moisture characteristic and hydraulic conductivity function. SWIM uses the equations of Campbell (1985) to define these functions. It requires the following inputs to parameterise these equations: θs, ψe, b and K_S. As described in Chapters 5 and 6, these variables were obtained for the top soil and subsoil respectively. The moisture characteristic for each layer was determined in the laboratory using pressure plates and a thermocouple psychrometer (Sections 5.2.2 and 6.2.1). Saturated hydraulic conductivity for the 0-18 cm, 18-24 cm and 24-36 cm layers was assumed to be equal to the hydraulic conductivity measured using a disc permeameter at 10 mm tension as described in Section 5.2.3. Saturated hydraulic conductivity for the subsoil layers was measured with a well permeameter (Section 6.2.2). Previous research has indicated that the effects of trafficking by sheep is limited to within the top 30 cm of soil (Lemin, 1992). It is therefore reasonable to assume that the subsoil hydrological properties under zero and low stocking intensities are the same. Drainage beneath the bottom layer (i.e. below 150 cm depth) was assumed to be due to gravity only.

Each simulation was run over a 48 hour period. In this time it was assumed that no transpiration or evaporation occurred.

Crust conductance is defined by the following equation:

$$\text{conductance} = K_S/dx \qquad [8.1]$$

where K_S = saturated hydraulic conductivity of a crust

dx = the thickness of a soil layer which may impede water entry

If the soil does not exhibit surface crusting, then the conductance value would be set so that the K_S of the crust is well above the K_S of the first soil layer. The precipitation constant determines the rate of exponential decrease in surface conductance with rainfall and the effectiveness parameter specifies the relation between rainfall energy and intensity (Ross, 1990). SWIM can also simulate a surface crust being present but not changing with rainfall by setting the initial and minimum conductance at the same value. For the gleyed podzolic soil at Big Ridge 1 it was assumed that there was no surface crusting and that the conductance of the soil surface did not change over the simulation period. The precipitation constant and the effectiveness parameter were set at SWIM default values.

The precipitation constant in the runoff parameter menu determines the rate of exponential decrease in surface storage with rainfall energy. It was assumed that soil surface storage did not change during the simulation time, hence the initial and minimum soil surface storage values are the same. The runoff rate factor and the runoff rate power combine to determine overland flow of water. The runoff rate factor and runoff rate power were set at 2, simulating a flat surface (H. Cresswell, *pers. comm.*). Each simulation was repeated using a runoff rate factor equal to 50. Here all water that exceeds the depressional storage runs off, none of which gets slowed up by runoff water that is slow to get away. Initial surface water depth accounts for any water present on the soil surface at the start of the simulation.

The initial input values for the SWIM model (Table 8.1) were changed from the base values to examine the effect of rainfall intensity, initial matric potential and depressional storage on the soil water balance of two grazing treatments. Different rainfall events can be simulated by SWIM, allowing the effects of storm events on the soil water balance under grazing to be examined. The initial matric potential of the soil results in changes to the soil water content which in turn effects infiltration and runoff. Depressions that store water on the soil surface are affected by grazing animals. Simulations were also carried out to examine the effects of changes in depressional storage on the soil water balance.

8.2.2 Effects of changing input values

8.2.2.1 Effects of designed storms

The probability of certain rainfall events in the Armidale district was calculated using the method given by Pilgrim (1987). The maximum intensities of storms that could be expected every 2, 10, 20 and 100 years were calculated (Table 8.2). A common rainfall pattern in the Armidale district is steady rainfall over two days. Using Pilgrim's (1987) method the intensity of rain falling for a duration of 48 hours was also calculated.

Table 8.2: Types of storms expected in the Armidale district over different time periods (Pilgrim, 1987)

	Average rainfall intensity		
Average recurrence interval	**1 hour duration**	**48 hour duration**	
(years)	**(mm/hr)**	**(mm/hr)**	**(mm/48 hrs)**
2 years	25	1.9	91.2
10 years	37	2.5	120
20 years	43	2.9	139.2
100 years	58	4.1	196.8

SWIM simulations were run for both grazing treatments using inputs from Table 8.1 for each of the storms shown in Table 8.2 (i.e. both 1 hour and 48 hour duration storms). Simulations were also run for storms with 70, 80, 90 and 100 mm of rain falling within the first hour. The simulations covered a period of 48 hours. Simulations were run with a runoff rate factor equal to 2 and to 50.

8.2.2.2 Effects of initial matric potential on simulated runoff

The above simulations were carried out using an initial matric potential equal to -100 cm H_20 (-10 kPa). The soil water content at this potential is commonly taken to be field capacity. To examine the effect of initial matric potential on runoff, simulations were run with an initial matric potential set at -200, -300, -400, -500, -600, -700, -800, -900 and -1000 cm H_20, for both grazing treatments. It was assumed that 100 mm of rain fell in the first hour of a 48 hour simulation. To assess the sensitivity of runoff to initial matric potential a rainfall intensity was chosen which ensured that some runoff would occur. Simulations were run with a runoff rate factor equal to 2 and to 50.

8.2.2.3 Effects of depressional storage on the soil water balance

To assess the effect of micro-relief on the soil water balance, depressional storages on the soil surface of 1, 1.5, 2 and 3 mm were used in four simulations. Simulations were again run for 48 hours with 100 mm of rain falling in the first hour, with a runoff rate factor equal to 2 and also to 50.

8.2.3 Sensitivity analysis

A linear sensitivity analysis was carried out to examine the sensitivity of SWIM to changes in input parameters. This was done by changing soil, runoff and conductance separately whilst keeping all other inputs at the specified base values given in Table 8.1. Values for these variables were increased or decreased by 10 per cent for the sensitivity simulations. Changes to the soil parameters were made to each layer in the soil profile. Rainfall was set at 100 mm falling during the first hour. The simulations ran for 48 hours and again it was assumed that there was no evapotranspiration loss during that time.

8.3 Results and discussion

8.3.1 Effects of designed storms on the soil water balance

The effect of storm events on the soil water balance for the two grazing treatments are shown in Table 8.3. With increasing rainfall intensity runoff is increased under both treatments. However, the amount of runoff is lower under the zero graze treatment. Rainfall intensity has relatively little effect on drainage under the conditions of these simulations.

Storm events are likely in the Armidale district over the summer. However, the SWIM simulations indicate that at least 70 mm of rain need to fall within one hour before runoff will occur (Table 8.3). According to Pilgrim (1987) this type of storm is unlikely in the Armidale district. Pilgrims (1987) average recurrence interval (ARI) calculations are based on a fairly short history of rainfall, no more than around 100 years, thus, the estimate of a 1 in 100 year ARI is not based on a long record in a relative sense. Therefore, the ARI's only provide an approximation of the type of storm event expected.

Table 8.4 shows the effect of steady rain falling continuously over a 48 hour period on the soil water balance. A larger total amount of rain fell over the 48 hours, but at a much lower intensity than for the one hour storms.

Table 8.3: The effect of rainfall intensity on the soil water balance[a, b]

(a) zero graze treatment

	Rainfall intensity (mm/hr)								
Water balance component (mm)	20 (1:1)	25 (1:2)	37 (1:10)	43 (1:20)	58 (1:100)	70	80	90	100
Runoff	0	0	0	0	0	0.03	1.9	8.2	16.8
Infiltration	20	25	37	43	58	69.97	78.1	81.8	83.2
Drainage	11	12	16	19	21	22	22	22	22
Profile water content	651	655	662	666	678	690	698	701	702

(b): 10 DSE/ha treatment

	Rainfall intensity (mm/hr)								
Water balance component (mm)	20 (1:1)	25 (1:2)	37 (1:10)	43 (1:20)	58 (1:100)	70	80	90	100
Runoff	0	0	0	0	0	0.75	5.8	13.9	22.9
Infiltration	20	25	37	43	58	69.25	74.2	76.1	77.1
Drainage	13	15	19	20	22	22	22	22	22
Profile water content	656	660	667	672	686	697	701	703	704

[a] All rain falls within the first hour and the simulation runs for 48 hours
[b] Values in brackets indicate the type of storms expected every 1, 2, 10, 20 and 100 years

Table 8.4: The effect of continuous, low intensity rainfall on the soil water balance for the two grazing treatments[a, b]

	Rainfall intensity (mm/hr)							
	1.9 (1:2)		2.5 (1:10)		2.9 (1:20)		4.1 (1:100)	
Water balance component (mm)	Zero graze	10 DSE/ha	Zero graze	10 DSE/ha	Zero graze	10 DSE/ha	Zero graze	10 DSE/ha
Runoff	0	0	4.7	9.8	22.8	28.2	78.3	84.0
Infiltration	91.2	91.2	110	105	111	105	112	107
Drainage	14	16	16	17	16	18	18	19
Profile water content	719	724	736	737	736	737	736	737

[a] The rain falls at the stated intensities for 48 hours and the simulation runs for 48 hours
[b] Values in brackets indicate the type of storms expected every 2, 10, 20 and 100 years

Continuous, low intensity rainfall will result in runoff from both grazing treatments when 2.5 mm of rain falls within each hour over a 48 hour duration. This type of rainfall event is more common in the district compared with the runoff producing high intensity storm. These two different rainfall events, high intensity/short duration and low intensity/long duration, affect infiltration and runoff in different ways.

For a storm event of high intensity and short duration, soil surface hydraulic conductivity has a major effect on runoff as it controls the flux of water entering the soil. Once rainfall intensity exceeds the soil conductance, runoff will occur. The zero graze treatment has a much higher hydraulic conductivity at the soil surface than the grazed treatment, allowing a greater quantity of water to infiltrate, resulting in less runoff. This is consistent with the work of other researchers (Dadkhah and Gifford, 1980; Willatt and Pullar, 1983; Proffitt *et al.*, 1993). Treading by grazing animals reduces macroporosity, resulting in decreased infiltration. Proffitt *et al.* (1993) found that infiltration was reduced due to the breakdown of the surface structure of a red-brown earth by sheep grazing during wet periods. Measurement of surface hydraulic properties in Chapter 5 show that the effects of compaction occur close to the soil surface. Although there were no significant differences in the moisture characteristic between grazing treatments at the 5-9 cm or 20-24 cm depths, the surface hydraulic conductivity was significantly reduced by grazing.

Under steady rainfall, the rainfall intensity is low but it may last for several hours. The low intensity allows rainfall to infiltrate until the surface horizons become saturated. In the duplex soil at Big Ridge the sandy clay loam A horizon overlies a medium to heavy clay B horizon. This dense B horizon has a much lower hydraulic conductivity than the A horizon (Table 8.1), impeding entry of water which is rapidly moving through the A horizon. As a result, the water content of the A horizon gradually increases until it reaches saturation. Further rainfall results in runoff as the soil is unable to hold any more water. Table 8.4 shows that runoff will occur under both treatments in a rainfall event which Pilgrim (1987) expects to occur once every ten years. Again, runoff from the zero graze treatment is lower than that from the grazed treatment. This is thought to be the result of greater numbers of macropores at the soil surface allowing more water to infiltrate.

Water ponding on top of the B horizon may occur during some rainfall events due to the low hydraulic conductivity of the B horizon compared to the A horizon. The occurrence of saturated conditions on top of the B horizon is likely to result in lateral water flow, especially where there is some slope. This water will move down slope taking with it nutrients and possibly soil particles. Lateral water movement within a dispersable soil can cause tunnel erosion. SWIM does not account for lateral flow, modelling vertical water movement only. If lateral water movement was significant, actual infiltration may be higher, as the A horizon is less likely to fully saturate with water draining away laterally across the top of the B horizon.

Rainfall intensity was found to have little effect on drainage. The hydraulic properties of the subsoil affect the amount of drainage and, given that these are the same for each treatment, there is no real difference in drainage between treatments. There is a small increase in drainage as rainfall intensity increases; however, this is due to the higher quantity of water available for infiltration.

In the field, runoff can be expected on the 15 and 20 DSE per ha plots on Big Ridge 1 with rainfall intensities greater than 25 mm per hour, and on the 10 DSE per ha plot with intensities greater than around 30 mm per hour (D. Wilkinson, *pers. comm.*). The reason why SWIM predicts that an intensity of at least 70 mm per hour is required before runoff will occur is due to the high K_S value measured at the soil surface using a disc permeameter. Hydraulic conductivity measurements were taken on Big Ridge 2, on a gleyed podzolic soil type using a drip infiltrometer (Section 2.4.2.2). On a grazed plot comparable to Plot 1, Big Ridge 1, the average hydraulic conductivity was 19.5 mm per hour (H. Cresswell, *pers. comm.*), compared to 71.9 mm per hour as measured with a disc permeameter on Big Ridge 1. Simulations were run using drip infiltrometer measurements of infiltration and are discussed in Section 8.3.1.2.

Vegetation on the soil surface has important consequences with regards to the soil water balance. Overland flow is slowed by vegetation on the soil surface, thus allowing more time for water to infiltrate. The detachment and movement of soil particles by the process of erosion is also inhibited.

Vegetation protects the soil surface, preventing crust development in soils with poor aggregate stability. The impact of raindrops can cause soil aggregates to breakdown into constituent particles (Rosewell *et al.*, 1991). These small particles are then washed down into soil surface pores thus blocking them. On drying, a surface crust develops which impedes infiltration. A vegetative cover on the soil surface will intercept raindrops reducing their impact. No surface crusting was observed on the experimental plots at Big Ridge 1. But, with high intensity rainfall, rapid entry of water and surface saturation, some slaking may occur resulting in decreased infiltration. This would be most likely where vegetative cover had been depleted by grazing.

Another ground cover effect is the interception of rainfall by vegetation. A proportion of the rain falling will not hit the ground but be intercepted by vegetation and remain on the leaves of plants until it eventually evaporates. Therefore, the actual rainfall available for infiltration is reduced depending on the vegetative cover.

Although the SWIM simulations presented in this study do not consider these effects of vegetation on the soil surface (due to the short simulation time of 48 hours) much research has emphasised the importance of ground cover in retarding runoff. Rauzi and Hanson (1966) examined the effects of grazing and vegetation cover on water infiltration and runoff. Infiltration was reduced and runoff increased with increased stocking rate. The differences between grazed and ungrazed treatments were due to altered soil structure, kind and amount of vegetation and natural mulch on the soil surface. Alderfer and Robinson (1947) suggested that the high rate of runoff from heavily grazed sites was due not only to a deterioration of soil physical properties at the soil surface, but also due to a lack of ground cover. Lang and McCaffrey (1984) found that ground cover impeded runoff, thereby reducing the amount of erosion. A critical ground cover of around 75 per cent in terms of runoff and erosion hazard is now a commonly accepted value for Australian conditions (Lang and McCaffrey, 1984).

8.3.1.1 Effects of designed storms on the soil water balance with SWIM's runoff rate factor equal to 50

Values of 2 for the runoff rate factor and runoff rate power parameters are appropriate for runoff from a flat surface (H. Cresswell, *pers. comm.*). The plots on Big Ridge 1 are relatively flat (< 5 % slope). Slope obviously affects runoff and the greater the slope the higher the runoff rate power and factor. However, there is no reliable information on the relationship between these two factors. The lack of predicted runoff at low intensity rainfall could be due to SWIM modelling a perfectly flat surface on which the excess water is ponded. By the end of the 48 hour simulation time, this ponded water has had time to infiltrate, hence no runoff occurs. Had there been a greater slope, the excess water would not have ponded, but would have been lost as runoff.

Table 8.5 and 8.6 show the effect of rainfall events on the soil water balance when the runoff rate factor is set at 50 for both treatments ensuring that all water that exceed the surface depressional storage runs off.

A rainfall intensity of at least 70 mm/hr is still required before runoff occurs (Table 8.5), but the amount of runoff is greater for both treatments, reflecting better what is observed in the field. Under low intensity, continuous rainfall the amount of runoff is also higher (Table 8.6) compared with the simulations which had a runoff rate factor of 2 (Table 8.4).

Table 8.5: The effect of rainfall intensity on the soil water balance, Runoff rate factor = 50[a,b]

(a) zero graze treatment

	Rainfall intensity (mm/hr)								
Water balance component (mm)	20 (1:1)	25 (1:2)	37 (1:10)	43 (1:20)	58 (1:100)	70	80	90	100
Runoff	0	0	0	0	0	0.5	6.3	14.5	23.6
Infiltration	20	25	37	43	58	69.5	73.7	75.5	76.4
Drainage	11	12	16	19	21	22	22	22	22
Profile water content	651	655	662	666	678	689	694	695	696

(b): 10 DSE/ha treatment

	Rainfall intensity (mm/hr)								
Water balance component (mm)	20 (1:1)	25 (1:2)	37 (1:10)	43 (1:20)	58 (1:100)	70	80	90	100
Runoff	0	0	0	0	0	3.8	11.6	20.6	29.9
Infiltration	20	25	37	43	58	66.2	68.4	69.4	70.1
Drainage	13	15	19	20	22	22	22	22	22
Profile water content	656	660	667	672	686	694	696	697	697

[a] All rain falls within the first hour and the simulation runs for 48 hours

[b] Values in brackets indicate the type of storms expected every 1, 2, 10, 20 and 100 years

Table 8.6: The effect of continuous, low intensity rainfall on the soil water balance for the two grazing treatments, Runoff rate factor = 50[a, b]

	Rainfall intensity (mm/hr)							
	1.9 (1:2)		2.5 (1:10)		2.9 (1:20)		4.1 (1:100)	
Water balance component (mm)	Zero graze	10 DSE/ha	Zero graze	10 DSE/ha	Zero graze	10 DSE/ha	Zero graze	10 DSE/ha
Runoff	0	0	7.1	12.3	25.6	31.0	81.7	87.4
Infiltration	91.2	91.2	110	105	111	105	112	107
Drainage	14	16	16	17	16	18	18	19
Profile water content	719	724	736	737	736	737	736	737

[a] The rain falls at the stated intensities for 48 hours and the simulation runs for 48 hours
[b] Values in brackets indicate the type of storms expected every 2, 10, 20 and 100 years

8.3.1.2 Effects of designed storms on the soil water balance using drip infiltrometer determined saturated hydraulic conductivity (K_s)

SWIM simulations were carried out using inputs given in Table 8.1, but replacing surface saturated hydraulic conductivity with the K_S measured with the drip infiltrometer. The results of the simulations are presented in Table 8.7. The effect of increasing rainfall intensity on the soil water balance was examined and compared with the simulations using K_S measured with a disc permeameter. The rainfall intensities are given in Table 8.2. Runoff was predicted at rainfall intensities of 43 mm per hour. The amount of runoff at higher rainfall intensities was greater than those simulated using K_S measured by the disc permeameter. Runoff was greater still when the runoff rate factor was set at 50 (Table 8.7b).

Although the disc permeameter is commonly used to measure hydraulic conductivity, the wetting mechanism is quite different from that of a drip infiltrometer, which is more similar to rainfall. The soil surface was found to be hydrophobic during the initial stages of wetting under the drip infiltrometer. This natural water repellence is overcome using a disc permeameter as the ground is wetted for a longer time. Water repellence could significantly increase the shedding of rainfall, at least in the early stages of a rain storm. Other reasons for higher K values measured using a disc permeameter is that wetting occurs under tension. Wetting is therefore slower and there is less breakdown of soil structure which commonly occurs under rainfall because of the impact from raindrops. Macroporosity is therefore preserved and infiltration is greater. The drip infiltrometer should also result in little surface disturbance as the drops have very low energy since they only fall a small distance before they hit the ground.

Table 8.7: The effect of rainfall intensity on the soil water balance using Ks at the soil surface which was measured with a drip infiltrometer, a) runoff rate factor =2, b) runoff rate factor =50[a,b]

a) Runoff rate factor =2

	Rainfall intensity (mm/hr)								
Water balance component (mm)	20 (1:1)	25 (1:2)	37 (1:10)	43 (1:20)	58 (1:100)	70	80	90	100
Runoff	0	0	0	0.003	3.7	11.5	19.5	28.1	37.1
Infiltration	20	25	37	42.99	54.3	58.5	60.5	61.9	62.9
Drainage	12	14	18	20	21	22	22	22	22
Profile water content	657	660	668	672	682	686	688	689	691

b) Runoff rate factor =50.

	Rainfall intensity (mm/hr)								
Water balance component (mm)	20 (1:1)	25 (1:2)	37 (1:10)	43 (1:20)	58 (1:100)	70	80	90	100
Runoff	0	0	0	0.056	9.4	19.6	28.7	38.1	47.7
Infiltration	20	25	37	42.94	48.6	50.4	51.3	51.9	52.2
Drainage	12	14	19	20	21	21	21	21	21
Profile water content	657	660	668	672	677	679	679	680	680

[a] All rain falls within the first hour and the simulation runs for 48 hours
[b] Values in brackets indicate the type of storms expected every 1, 2, 10, 20 and 100 years

These simulations have identified two runoff mechanisms on the gleyed podzolic. If the drip infiltrometer hydraulic conductivity values are used, runoff will occur by Hortonian flow only in approximately a 1 in 20 year storm (Table 8.7). Hortonian flow occurs when the surface conductivity is less than the rainfall intensity, resulting in runoff even though the soil profile is not saturated. However, saturation excess runoff is likely at least 1 in 10 years (Table 8.4). Here the A horizon becomes saturated as the low hydraulic conductivity of the B horizon impedes water entry ultimately controlling infiltration. To improve infiltration and water availability for the pasture, and to reduce the potential for erosion and surface nutrient transport, the hydraulic properties of the B horizon need to be improved. This may involve deep ripping, although the creation of more pore space is only temporary. A more permanent measure would involve production of vigorously growing, deep rooted perennial plant species that will create biopores and increase faunal activity in the B horizon thus increasing the hydraulic conductivity.

8.3.2 Effects of initial matric potential on simulated runoff

Initial soil water potential and thus water content of the soil have important consequences on the amount of runoff, as illustrated in Figure 8.1. Runoff decreases sharply as the initial potential falls for both treatments, ceasing at an initial water potential of -49 kPa for the zero graze and -98 kPa for the 10 DSE/ha treatment. Runoff is greater with the runoff rate factor set to 50, ceasing at an initial matric potential of -59 kPa for the zero graze and at a potential lower than -98 kPa for the 10 DSE/ha treatment (Figure 8.2).

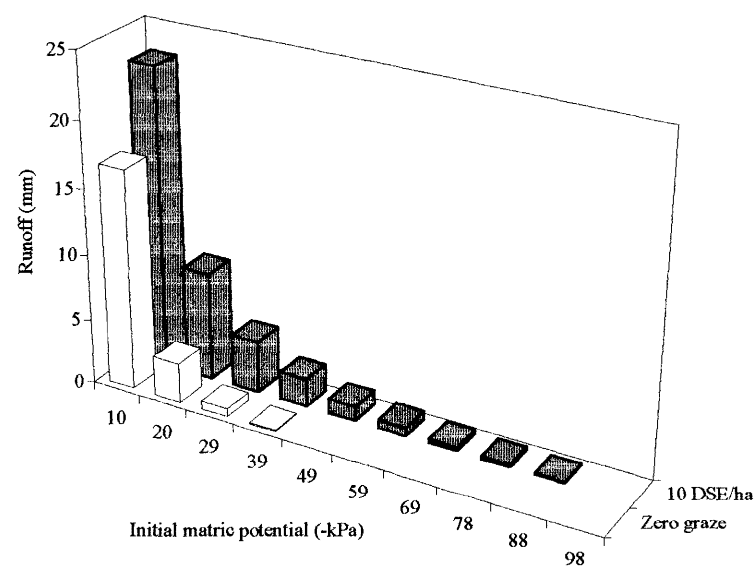

Figure 8.1: The effect of initial soil water potential and content on runoff during a rainfall event of 100 mm/hr received in the first hour of a 48 hour simulation

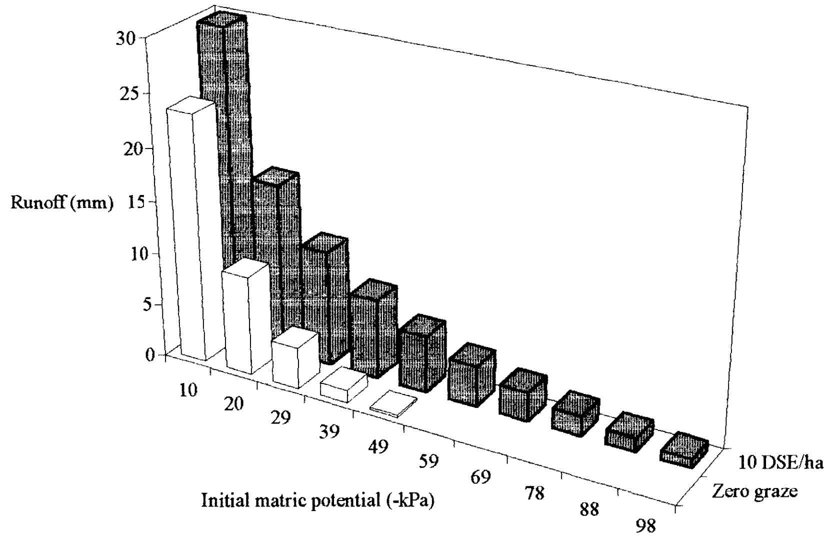

Figure 8.2: The effect of initial soil water potential and content on runoff during a rainfall event of 100 mm/hr received in the first hour of a 48 hour simulation, Runoff rate factor = 50

The field measured initial water contents of the 0-18 cm, 18-24 cm and 24-30 cm layers at the start of the simulations and the respective air-filled porosity's in the two grazing treatments are shown in Table 8.8. Air-filled porosity indicates the amount of air-filled pore space available in which the air can be displaced by infiltrating water, i.e. the volume in the A horizon that can be filled with water before full saturation occurs. Since water and air compete for the same pore space, a decrease in soil water content results in an increase in air-filled porosity and likewise an increase in soil water content reduces air-filled porosity. The zero-graze treatment has a higher air-filled porosity at each depth compared to the 10 DSE per ha resulting in increased infiltration, and therefore, reduced runoff.

Table 8.8: Water content and air-filled porosity at the start of the simulations

a) Zero graze

Depth	0-18 cm		18-24 cm		24-36 cm	
Initial matric potential (cm H20)l	Water content (m3 m-3)	Air-filled porosity (m3 m-3)	Water content (m3 m-3)	Air-filled porosity (m3 m-3)	Water content (m3 m-3)	Air-filled porosity (m3 m-3)
-100	0.337	0.146	0.298	0.132	0.277	0.149
-200	0.286	0.197	0.258	0.172	0.247	0.179
-400	0.243	0.240	0.223	0.207	0.219	0.207
-600	0.221	0.262	0.205	0.225	0.205	0.221
-800	0.206	0.277	0.193	0.237	0.195	0.231
-1000	0.196	0.287	0.185	0.245	0.188	0.238

b) 10 DSE per ha

Depth	0-18 cm		18-24 cm		24-36 cm	
Initial matric potential (cm H20)l	Water content (m3 m-3)	Air-filled porosity (m3 m-3)	Water content (m3 m-3)	Air-filled porosity (m3 m-3)	Water content (m3 m-3)	Air-filled porosity (m3 m-3)
-100	0.334	0.150	0.304	0.113	0.342	0.096
-200	0.291	0.193	0.270	0.147	0.313	0.125
-400	0.254	0.230	0.239	0.178	0.286	0.152
-600	0.234	0.250	0.223	0.194	0.272	0.166
-800	0.221	0.263	0.212	0.205	0.262	0.176
-1000	0.211	0.273	0.204	0.213	0.255	0.183

Infiltration and runoff are important as they influence the potential amount of water available for plant growth and because runoff is the driving force behind soil erosion. Several soil factors affect the amount of infiltration and therefore runoff, including the soil's initial water potential and thus water content. As the soil dries, runoff is reduced as a result of increased infiltration. The duplex nature of the gleyed podzolic results in water movement being retarded due to the dense clay B horizon. Drainage through the overlying A horizon is also impeded by the B horizon. As a result, the soil will take some time to dry after a rainfall event. Further rainfall may result in runoff occurring due to the high moisture content of the soil profile.

8.3.3 Effects of depressional storage on the soil water balance

Table 8.9 shows the effect of soil surface water storage on the soil water balance. An increase in surface detention reduces the amount of runoff and increases infiltration. The results of this simulation with a runoff rate factor equal to 50 are shown in Table 8.10.

Table 8.9: The effect of soil surface detention on runoff, infiltration and drainage[a]

	Runoff (mm)		Infiltration (mm)		Drainage (mm)	
Surface Detention (mm)	Zero graze	10 DSE/ha	Zero graze	10 DSE/ha	Zero graze	10 DSE/ha
1 mm	17.7	23.9	82.3	76.1	22	22
1.5 mm	17.2	23.4	82.8	76.6	22	22
2 mm	16.8	22.9	83.2	77.1	22	22
3 mm	15.8	22.0	84.2	78.0	22	22

[a] 100 mm of rain fell within the first hour and the simulation ran for 48 hours

Table 8.10: The effect of soil surface detention on runoff, infiltration and drainage, Runoff rate factor = 50[a]

	Runoff (mm)		Infiltration (mm)		Drainage (mm)	
Surface Detention (mm)	Zero graze	10 DSE/ha	Zero graze	10 DSE/ha	Zero graze	10 DSE/ha
1 mm	24.6	30.9	75.4	69.1	22	22
1.5 mm	24.1	30.4	75.9	69.6	22	22
2 mm	23.6	29.9	76.4	70.1	22	22
3 mm	22.6	28.9	77.4	71.1	22	22

[a] 100 mm of rain fell within the first hour and the simulation ran for 48 hours

Undulations and depressions on the soil surface increase the storage capacity of water on the soil surface and slows down overland flow. This allows ponded water to infiltrate later reducing the amount of runoff (Moore and Larson, 1979; Warren *et al.*, 1986a). The micro-relief of agricultural soils varies according to land use and is constantly being modified by rainfall and wind (Moore and Larson, 1979).

Moore and Larson (1979) identified three stages which occur during a rainfall event with regard to micro-relief and runoff. Firstly, as rainfall intensity starts to exceed the infiltration rate, water begins to be stored in the depressions on the soil surface, with no runoff occurring. Next, more rainfall further fills surface storages and some runoff will also begin to occur. Finally, surface storage is at a maximum and only runoff occurs. Once the rain stops, these stages will occur in reverse.

Although it has been found in several studies that micro-relief significantly affects infiltration and runoff (Moore and Larson, 1979; Warren *et al.*, 1986a; Eldridge, 1991), there is little research into the effects of trampling on micro-relief. Most work has examined the effect of cultivation on micro-relief (Kuipers, 1957; Burwell *et al.*, 1963; Moore and Larson, 1979). Warren *et al.* (1986b) examined the effects of livestock treading on several properties, including micro-relief, of a silty clay soil. They found that although the action of the hoof on the soil surface resulted in a breakdown of soil aggregates, there was no significant correlation between micro-relief and grazing intensity.

Edmond (1962) and Mullen *et al.* (1974) found treading increased soil surface roughness, particularly when the soil was moist. Given that a soil is most susceptible to compaction when it is wet, the depressions formed by animal treading may actually have a compacted base that can decrease infiltration.

The simulations show that changed hydrological properties due to grazing results in decreased infiltration, which leads to increased runoff. However, a stocking rate of 10 DSE per ha has not degraded the soil structural condition enough to induce runoff under more common rainfall events. Grazing effects are pronounced during wet seasons or storm events which produce more than 43 mm of rain in an hour.

8.3.4 Sensitivity analysis

The sensitivity of SWIM output to changes in the soil input parameters is shown in Table 8.11. Runoff is highly sensitive to initial matric potential (ψm), saturated water content (θs), air-entry potential (ψe) and parameter b (slope of the best fit line relating θ to ψ on a log-log scale). A 10 per cent change in saturated water content and b lead to a significant change in infiltration and runoff.

Table 8.11: The sensitivity of the SWIM model's output to changes in values of soil input parameters[a]

Input[b]	Change in input	Runoff (mm)		Infiltration (mm)		Drainage (mm)		Profile water content (mm)	
Initial ψm	+10%	26.2	(14.4)	73.8	(-4.3)	22.6	(1.8)	707.4	(0.5)
	-10%	20.2	(-11.8)	79.8	(3.5)	21.9	(-1.4)	701.1	(-0.4)
θs	+10%	17.7	(-22.7)	82.3	(6.7)	22.0	(-0.9)	774.8	(10.0)
	-10%	28.7	(25.3)	71.3	(-7.5)	22.4	(0.90)	632.4	(-10.2)
ψe	+10%	20.5	(-10.5)	79.5	(3.1)	21.7	(-2.3)	700.3	(-0.6)
	-10%	25.4	(10.9)	74.6	(-3.2)	22.6	(1.8)	707.5	(0.5)
b	+10%	27.4	(19.7)	72.6	(-5.8)	22.4	(0.9)	706.8	(0.4)
	-10%	17.1	(-25.3)	82.9	(7.5)	21.9	(-1.4)	700.6	(-0.51)
Ks	+10%	22.1	(-3.5)	77.9	(1.0)	24.6	(10.8)	702.6	(-0.2)
	-10%	23.9	(4.4)	76.1	(-1.3)	19.8	(-10.8)	705.6	(0.1)

[a] The values in brackets are the percentage changes due to a 10 per cent increase or decrease in the base values of SWIM inputs.
[b] ψm is matric potential, θs saturated water content, ψe the air-entry potential, *b,* the slope of the best fit line relating θ to ψ on a log-log scale and Ks saturated hydraulic conductivity.

When the initial matric potential input is changed, the simulation will start at different points on the K(θ) function and the moisture characteristic. This results in different suction gradients and different air-filled porosity's available to store water. A 10 per cent increase in initial matric potential resulted in a extra 3 mm of water running off and therefore, infiltration was reduced by 3 mm (Table 8.11). An increase in initial matric potential means that the soil is holding more water and is nearer to saturation. Therefore, there is less potential drawing water through the soil surface, hence a reduced infiltration rate. Drainage is insensitive to changes to initial matric potential, changing by less than 0.5 mm with either a 10 per cent increase or a 10 per cent decrease in initial matric potential. Changes in profile water content corresponded to the change in infiltration and runoff.

Saturated water content (θs) describes the total amount of water which a soil can hold. Runoff, infiltration and profile water content are all sensitive to changes in this parameter. The higher the θs value the more water a soil will hold, hence the greater quantity of water that can enter the soil before runoff occurs.

A change in saturated water content affects the moisture characteristic. As previously mentioned, SWIM uses Campbell's (1974) function to define the moisture characteristic for each layer. Saturated water content is an input required for Campbell's water retention function. A change in this parameters results in a parallel shift of the moisture characteristic from its original position (i.e. the slope remaining the same). Therefore, a shift to the left due to a 10 per cent decrease in saturated water content results in a decrease in the amount of water being held at any given potential. Whereas a shift to the right means an increase in water content at any given potential.

Runoff and infiltration are also sensitive to changes in the air-entry potential (ψe). As ψe is decreased, infiltration decreases and runoff increases. The air-entry potential refers to the potential at which the largest pores in the soil begin to drain. A change in ψe moves the soil moisture characteristic. If ψe is decreased, a greater suction must be exerted before the largest pores begin to drain. The soil therefore remains at a high water content for longer, which in turn affects infiltration and runoff.

The slope of the moisture characteristic (*b*) indicates the change in soil water content expected with a change in matric potential. A steep slope means that a given change in matric potential results in an even smaller change in water content. Whereas for a flatter moisture characteristic, a greater quantity of water will drain as matric potential decreases. A 10 per cent increase in the *b* value results in an extra 5 mm of water that runs off. As the soil holds more water at each potential, due to a higher *b* value, less water will infiltrate and consequently runoff will increase. When the *b* value is changed, both the moisture characteristic and the hydraulic conductivity function ($K(\theta)$) are modified as *b* is used in Campbell's (1974) hydraulic conductivity function.

Drainage is most sensitive to changes in saturated hydraulic conductivity (K_S) (Table 8.11). According to Darcy's law, hydraulic conductivity and potential gradient determines the rate at which water moves through the soil and thus the amount of water available for drainage.

SWIM output is relatively insensitive to variation in runoff inputs (Table 8.12). A 10 per cent change in surface storage lead to a less than 1 mm change in all components of the water balance. Cresswell *et al.* (1992) suggested that surface storage provides a buffering effect, allowing rainfall to exceed infiltration for short periods without runoff occurring. The runoff rate factor enables SWIM to account for some slope in the topography during the simulation. Obviously the greater the slope the easier it is for water to runoff, unlike on a flat surface where runoff water is often slow to get away. Given the insensitivity of SWIM to the runoff inputs, an error in determining these inputs will not make a great deal of difference to model output. This is particularly advantageous with regards to determining the runoff rate factor and the runoff rate power as they are difficult to determine.

Table 8.12: The sensitivity of the SWIM model's output to changes in values of runoff parameters[a]

Input	Change in input	Runoff (mm)		Infiltration (mm)		Drainage (mm)		Profile water content (mm)	
Surface storage	+10%	22.8	(-0.44)	77.2	(0.13)	22.2	(0.00)	704.4	(0.03)
	-10%	23.1	(0.87)	76.9	(-0.26)	22.2	(0.00)	704.0	(-0.03)
Runoff rate factor	+10%	22.9	(0.00)	77.1	(0.00)	22.2	(0.00)	704.2	(0.00)
	-10%	23.0	(-0.44)	77.0	(-0.13)	22.2	(0.00)	704.1	(-0.01)
Runoff rate power	+10%	23.3	(1.75)	76.7	(-0.52)	22.2	(0.00)	703.8	(-0.06)
	-10%	22.6	(-0.01)	77.4	(0.39)	22.2	(0.00)	704.5	(0.04)

[a] The values in brackets are the percentage change in SWIM output due to a 10 per cent increase or decrease in the base values of SWIM inputs.

SWIM output is insensitive to changes in surface conductance (Table 8.13). It was assumed that there was no decrease in surface conductance over the simulation period. If the soil surface had poor structure with crusting developing during rainfall, the models output is likely to have been more sensitive to the conductance parameters.

Table 8.13: The sensitivity of the SWIM model's output to changes in values of conductance parameters[a]

Input	Change in input	Runoff (mm)		Infiltration (mm)		Drainage (mm)		Profile water content (mm)	
Surface conductance	+10%	22.9	(0.00)	77.1	(0.00)	22.2	(0.00)	704.2	(0.00)
	-10%	22.9	(0.00)	77.1	(0.00)	22.2	(0.00)	704.2	(0.00)

[a] The values in brackets are the percentage change in SWIM output due to a 10 per cent increase or decrease in the base values of SWIM inputs.

The sensitivity analysis is only relevant to the specific conditions of the simulations carried out in this study. The sensitivity of model output to changes in input parameters will vary with different soil types, climatic data such as rainfall events and with different types of vegetation.

8.4 Conclusion

Changes in surface hydraulic properties as a result of animal grazing adversely affects the soil water balance. A loss of macroporosity at the soil surface under grazing results in reduced infiltration and an increase in the amount of runoff.

The simulations show that a stocking rate of 10 DSE per ha, on the gleyed podzolic at Big Ridge 1, has not degraded soil structural condition enough to induce runoff, even in quite severe storms for the Armidale area. However, the simulations show clearly that during a runoff producing rainfall event, runoff is much higher in the grazed plot compared to the ungrazed plot.

SWIM predicts that for short duration storms runoff does not occur until rainfall intensity reaches 70 mm/hr. Field observations have shown that runoff would occur on Big Ridge 1 at rainfall intensities less than this. The difference between simulated and observed runoff is most likely due to the high values of hydraulic conductivity at the soil surface which were measured using a disc permeameter and used in the SWIM simulations. Drip infiltrometer measurements of hydraulic conductivity were lower than those measured with the disc permeameter and the simulations using the drip infiltrometer measurements were closer to field observations.

Low intensity rainfall lasting for several hours is a more common rainfall pattern experienced in the Armidale area. Under this type of rainfall SWIM predicted runoff from a 1 in 10 year rainfall event.

Simulation modelling has identified two runoff mechanisms on the gleyed podzolic soil, namely, runoff by Hortonian flow and saturation excess runoff. Runoff by Hortonian flow was predicted to occur during about a 1 in 20 year storm event, whereas saturation excess runoff is likely at least once every 10 years. Therefore, the saturation excess runoff mechanism is more likely to occur, even on soils grazed at 10 DSE per ha.

Low intensity rainfall allows water to steadily infiltrate into the sandy clay loam A horizon of the gleyed podzolic. The medium to heavy clay B horizon has a low hydraulic conductivity which restricts water entry from the A horizon. The A horizon will therefore become saturated and further rainfall runs off. The B horizon controls infiltration and therefore, improvements to the hydraulic properties of the B horizon would be required to reduce the occurrence of saturated excess runoff.

Changes in initial matric potential affect the soil water balance. Infiltration is reduced with increasing matric potential. This is due to a reduction in air filled pores as the soil water content is higher. A soil with a low air-filled porosity will saturate more quickly than one with a high air-filled porosity. Given that the 10 DSE per ha treatment has a lower air-filled porosity at the soil surface compared to the zero graze treatment, the amount of water it can absorb will be less increasing the probability of runoff.

Soil surface storage will slow down overland flow and allow more time for ponding water to infiltrate, reducing the amount of runoff.

The sensitivity analysis shows that SWIM output is most sensitive to changes to the soil inputs. This is to be expected since all of the soil inputs are used to solve Richards' equation, which describes water movement through the soil profile. Accurate measurement of soil hydraulic properties is crucial for reliable model output. This requires fast efficient measurement techniques along with a greater understanding of the spatial variability of hydraulic properties.